THE JOURNAL OF BIOLOGICAL CHEMISTRY
Vol. 279, No. 32, Issue of August 6, pp. 33816–33828, 2004

Printed in U.S.A.

The LFA-1-associated Molecule PTA-1 (CD226) on T Cells Forms a Dynamic Molecular Complex with Protein 4.1G and Human Discs Large*

Received for publication, January 30, 2004, and in revised form, April 14, 2004
Published, JBC Papers in Press, May 11, 2004, DOI 10.1074/jbc.M401040200

Kylie J. Ralston‡, Samantha L. Hird‡, Xinhai Zhang‡, Judith L. Scott‡, Boquan Jin§, Rick F. Thorne‡¶, Michael C. Berndt‖, Andrew W. Boyd, and Gordon F. Burns‡ ‡‡**

*From the ‡Cancer Research Unit, School of Biomedical Sciences, The University of Newcastle, University Drive, Callaghan, New South Wales 2308, Australia, the §Department of Immunology, The 4th Military Medical University, Xi'an 710032, People's Republic of China, the ‖Department of Biochemistry and Molecular Biology, Monash University, Clayton, Victoria 3168, Australia, and the **Division of Cancer and Cell Biology, Queensland Institute of Medical Research, Royal Brisbane Hospital PO, Brisbane, Queensland 4029, Australia*

Clustering of the T cell integrin, LFA-1, at specialized regions of intercellular contact initiates integrin-mediated adhesion and downstream signaling, events that are necessary for a successful immunological response. But how clustering is achieved and sustained is not known. Here we establish that an LFA-1-associated molecule, PTA-1, is localized to membrane rafts and binds the carboxyl-terminal domain of isoforms of the actin-binding protein 4.1G. Protein 4.1 is known to associate with the membrane-associated guanylate kinase homologue, human discs large. We show that the carboxyl-terminal peptide of PTA-1 also can bind human discs large and that the presence or absence of this peptide greatly influences binding between PTA-1 and different isoforms of 4.1G. T cell stimulation with phorbol ester or PTA-1 cross-linking induces PTA-1 and 4.1G to associate tightly with the cytoskeleton, and the PTA-1 from such activated cells now can bind to the amino-terminal region of 4.1G. We propose that these dynamic associations provide the structural basis for a regulated molecular adhesive complex that serves to cluster and transport LFA-1 and associated molecules.

A successful immunological response requires the activation, proliferation, and differentiation of T cell subsets into effector cells. These events are initiated by signals generated by sustained interaction between T cell receptors (TCR)[1] and antigen-presenting cells (APC), together with the engagement of accessory counter receptors between the T cell and APC. Without the coordinated engagement of accessory receptors, engagement of the TCR can result in T cell anergy (1). Receptor engagement and signaling appear to be coordinated, both temporarily and spatially, at a specialized region known as the immunological synapse (2, 3) increasingly recognized as containing structural elements shared with classical neuronal synapses (4, 5).

Crucial to the formation of the immunological synapse are specialized membrane microdomains known as rafts (6) and also the rearrangement of elements of the cytoskeleton. Both of these essential components are influenced by receptor engagement at the synapse, and, in turn, both orchestrate molecular distribution and signal transduction during the interaction (7–9). An initiating event in synapse formation may be the migration of intercellular adhesion molecule 3 (ICAM-3) to sites of cell-cell contact with the APC, where it engages its counter receptor as part of the "scanning" process (10). Engagement of ICAM-3 results in an increase in intracellular calcium concentration, the activation of tyrosine kinases, and activation of the integrin LFA-1 (10, 11). The mechanisms involved in such "inside-out" activation of leukocyte integrins are complex and not fully understood (12, 13), but changes in avidity and affinity of LFA-1 involve clustering in membrane rafts (14–16) and remodeling of the actin (9, 17) and microtubule (18, 19) cytoskeleton. Increased intracellular calcium concentration activates the small GTPase Rap1, emerging as a major stimulus for LFA-1 clustering and ligand binding (20–23). Calcium also activates calpain (24), the proteolytic enzyme that cleaves talin, a process required for the linkage between integrins and the actin cytoskeleton that contributes to their clustering and activation (24–27). Recently, Ginsberg's group demonstrated that a phosphotyrosine motif within a β turn of the integrin β subunit binds to the four point 1/ezrin/radixin/moesin (FERM) (28) domain contained in the talin head region and exposed by cleavage from the remainder of the molecule (27, 29).

Subsequently, the TCR and small accessory adhesion receptors migrate to the core of the synapse to form the central supramolecular activating complex, and larger molecules, including LFA-1 and associated talin, are displaced to an outer adhesive ring, the peripheral supramolecular activating complex (2, 30). These movements may be regulated in part by the greater numbers of small molecules simply displacing LFA-1

* This work was supported by a grant from the National Health and Medical Research Council of Australia and by National Natural Science Foundation of China Grant 30030130. The costs of publication of this article were defrayed in part by the payment of page charges. This article must therefore be hereby marked "*advertisement*" in accordance with 18 U.S.C. Section 1734 solely to indicate this fact.

¶ Supported by a Brawn Fellowship from the University of Newcastle. Present address: Breakthrough Breast Cancer Centre, Institute of Cancer Research, 237 Fulham Rd., Chelsea, London SW3-6JB, United Kingdom.

‡‡ To whom correspondence should be addressed. Tel.: 61-2-49217860; Fax: 61-2-49217867; E-mail: Gordon.Burns@newcastle.edu.au.

[1] The abbreviations used are: TCR, T cell receptor(s); APC, antigen-presenting cell; FERM, four point one ezrin radixin moesin; ERM, ezrin, radixin, moesin; MAGUK, membrane-associated guanylate kinase homologue; hDlg, human discs large; GEM, glycolipid-enriched membranes; GST, glutathione *S*-transferase; CTD, carboxyl-terminal domain; ATD, amino-terminal domain; ICAM, intercellular adhesion molecule; GAKIN, guanylate kinase-associated kinesin; mAb, monoclonal antibody; aa, amino acid(s); CHO, Chinese hamster ovary; RAM, rabbit anti-mouse immunoglobulin(s); MES, 4-morpholineethanesulfonic acid; PBS, phosphate-buffered saline; PKC, protein kinase C; TPA, 12-*O*-tetradecanoylphorbol-13-acetate.

and other larger molecules within rafts (30). However, larger adhesion molecules such as CD43, the presence of which might hinder TCR engagement on physical grounds, are actively excluded from the synapse by association with ERM proteins (31). The ERM proteins themselves participate in a number of processes essential to T cell activation, including the movement of adhesion receptors, membrane and cytoskeletal redistribution, and signal transduction (32–35). Members of an extended protein 4.1 superfamily, these proteins are characterized by their possession of a FERM domain toward the amino terminus and an F actin-binding segment at the carboxyl terminus: in the resting state, these regions form an intramolecular association that masks other associations, but following activation by threonine phosphorylation and binding of phosphoinositides, the tail region is able to extend to bind actin, and the FERM domain is exposed to bind the juxtamembrane region of any of several adhesion molecules, thereby providing a transmembrane linkage to the actin cytoskeleton (36–39).

The FERM domain of the prototypic protein 4.1R shares about 30% identity with that of the ERM family members (28) and shares the capacity to bind transmembrane proteins (40). In addition, however, this domain of protein 4.1 can bind to another class of proteins, the membrane-associated guanylate kinase homologues (MAGUKs) (41). MAGUK family members contain a number of protein-protein interactive domains, including Src homology 3 and PDZ domains, and serve to mediate the tight clustering of both transmembrane receptors and ion channels at sites of cell-cell communication such as neuronal synapses (42). Since the sequence of amino acids in the FERM domain of 4.1 that binds to transmembrane receptors can differ from that bound by MAGUKs, these molecules potentially can form a protein 4.1-transmembrane protein-MAGUK ternary complex to provide a functional unit at the plasma membrane with links to the cytoskeleton, and there are now several examples of such a clustering complex (41, 43). Furthermore, linkages between these complexes and the cytoskeleton may be more than passive, since several regulators of small GTPases contain residues conserved in the 4.1-MAGUK binding site (41, 44, 45).

Recent work from Chishti's laboratory has raised the exciting possibility that such a MAGUK complex might play a role in the formation of physical contacts between T cells and APC and in the regulation of T cell activation, thus extending the commonalities between the immunological synapse and classical neuronal synapses (46). This group first identified that in T cells the MAGUK, human discs large (hDlg), interacts with both the tyrosine kinase Lck and the potassium ion channel, Kv1.3 (47). Both Lck and Kv1.3 are known regulators of T cell signaling and adhesion that may localize to the immunological synapse (48–50), and hDlg translocates to the lymphocyte cap upon cross-linking of the CD2 receptor (46). hDlg also associates with a kinesin-like motor protein termed guanylate kinase-associated kinesin (GAKIN), an association with the potential to drive the microtubule-based trafficking of the complex to the plasma membrane (46, 51, 52). Moreover, in different cell types, both MAGUKs and members of the 4.1 family are able to bind transmembrane proteins, thus contributing to the scaffolding complex (41). In the present study, we identify a binding partner for the protein 4.1 paralogue, 4.1G, in T cells, the transmembrane protein PTA-1 (CD226). In addition, we demonstrate that PTA-1 can bind to hDlg in a process requiring its carboxyl-terminal peptide residues, which contain a PDZ-binding motif. We show that PTA-1 binds to the carboxyl-terminal domain of 4.1G, and the proteins associate under resting conditions, but, upon stimulation of Jurkat cells, PTA-1 now can bind to the amino-terminal region of 4.1G and the complex associates with the cytoskeleton.

PTA-1 (also known as CD226, TLiSA-1, and DNAM-1) is a member of the immunoglobulin superfamily, the expression of which is regulated by phorbol ester and calcium (53, 54). Initially identified as a T cell activation antigen, antibodies and $F(ab')_2$ fragments against PTA-1 inhibit the development of cytotoxic T cells and T cell clones from their precursors (55–57). PTA-1 was also identified on platelets where it may engage in signal transduction, since anti-PTA-1 monoclonal antibodies (mAbs) induce platelet activation and aggregation in a process that requires the Fc receptor (58). Recently Shibuya *et al.* (59) showed that PTA-1 was physically and functionally associated with LFA-1 in NK cells and activated T cells in a process requiring phosphorylation of a serine residue in the PTA-1 cytoplasmic tail. In addition, cross-linking of LFA-1 induced tyrosine phosphorylation of PTA-1, possibly mediated by Fyn with which PTA-1 also associates. Circumstantially, these findings place PTA-1 at the peripheral supramolecular activating complex of the immunological synapse during T cell activation and suggest that it may play a role in LFA-1 activation and downstream signaling. In this study, we additionally show that PTA-1 associates with Rap-1 in membrane fragments from activated T cells and that the complex of protein 4.1G, hDlg, and PTA-1 is contained within membrane rafts.

EXPERIMENTAL PROCEDURES

Antibodies—The LeoA1 (55) and FMU4 (60) mAbs are directed against PTA-1. Rabbit polyclonal antibodies to 4.1G were raised against GST fusion proteins containing the amino-terminal domain, 4.1G-Head (aa 1–115) and the carboxyl-terminal domain, 4.1G-Tail (aa 830–1005). Affinity-purified IgG was obtained using either GST-4.1G-Head or GST-4.1G-Tail conjugated to a 1:1 mixture of Affi-gel 10 and 15 (Bio-Rad) (1 mg of protein/10 ml of resin). Pooled antisera from multiple bleeds were loaded through the relevant column, and bound IgG was eluted with 0.1 M glycine, pH 2.4, immediately reneutralized with one-fifth volume of 1 M Tris, pH 8.0, and dialyzed against Tris saline buffer, pH 7.4. This affinity-purified antibody was then passed through a GST-Affi gel 10/15 column to remove IgG against the GST portion of the fusion protein. The mAb directed against hDlg (2D11) was a gift from Dr. M. Lutchman (Tufts University School of Medicine, Boston, MA). The VIIIA7 anti-DAF mAb was a gift from Dr. D. Shafren (Department of Microbiology and Immunology, University of Newcastle). The Rap1 and calnexin mAbs were purchased from BD Transduction Laboratories (Lexington, KY). The anti-CD3 mAb (OKT3) was purchased from ATCC.

Cell Lines and Establishment of Permanent Transfectants—The Jurkat T cell line (ATCC) was maintained in RPMI 1640 medium (Thermo Trace, Melbourne, Australia) containing 10% fetal bovine serum (CSL, Melbourne, Australia). PTA-1 cDNA was subcloned into the high expression level eukaryotic vector, pEF-BOS, as described previously (54). The permanent Jurkat-PTA-1 cell line was established using the LipofectAMINE™ 2000 reagent (Invitrogen) to introduce a 10:1 excess of the pEF-BOS-PTA-1 vector (which lacks a eukaryotic selection marker) to pREP9 (which encodes neomycin phosphotransferase; Invitrogen), followed by selection with 750 μg/ml G-418 (Invitrogen). The PTA-1-positive population was verified by flow cytometry and further enriched by fluorescence-activated cell sorting with the LeoA1 mAb.

The Chinese hamster ovary (CHO) cell line permanently transfected with PTA-1 (CHO-PTA-1) or DAF (CHO-DAF) were established as described above and maintained in Dulbecco's modified Eagle's medium (CSL, Melbourne, Australia) with 10% fetal bovine serum. The CHO-DAF cells were kindly provided by Dr. D. Shafren.

Isolation of Glycolipid-enriched Membranes (GEMs)—These were prepared as described previously (61). Briefly, Jurkat-PTA-1 cells ($\sim 7 \times 10^7$ cells/treatment) were treated with TPA (Sigma) at 50 ng/ml at 37 °C for varying times, as indicated, or cross-linked with either LeoA1 or control mAbs followed by rabbit anti-mouse immunoglobulins (RAM) (as described below). Whole cell lysates were solubilized in 1% Triton X-100 in MES-buffered saline, pH 6.5, adjusted to 40% sucrose and applied under a discontinuous 5–30% sucrose gradient. Following overnight ultracentrifugation, the GEMs separated as a low density light-refractive band. The soluble fraction and GEMs were collected; GEMs were washed and dissolved in MES-buffered

saline; and the insoluble pellet was further processed by washing with MES-buffered saline and centrifuged at 14,000 × *g* for 15 min at 4 °C, and then reducing Laemmli sample buffer was added to the pellet and boiled. Equal protein quantities (15 μg) of the GEM and soluble fractions, along with an equal proportion of the insoluble pellets, were separated on 7.5% SDS-PAGE and electrotransferred to nitrocellulose (Sartorius, Germany) using 25 mM Tris, 192 mM glycine, and 20% methanol transfer buffer. To visually determine equal protein loading, the nitrocellulose membrane was stained with Ponceau S (0.5% Ponceau S, 1% glacial acetic acid) and then washed with TTBS, followed by immunoblot analysis.

Immunoblotting—Nitrocellulose membranes were blocked in 5% skim milk in TTBS (25 mM Tris-HCl, pH 8.0, 144 mM NaCl, 0.05% Tween 20) before incubation with primary antibody in 1% skim milk/TTBS. Membranes were then incubated with horseradish peroxidase-conjugated goat anti-mouse or anti-rabbit immunoglobulins (Bio-Rad), and the immunocomplexes were detected by enhanced chemiluminescence. Between subsequent probes, membranes were stripped by incubation at 60 °C for 30–45 min with 62.5 mM Tris-HCl, pH 6.7, containing 100 mM 2-β-mercaptoethanol and 2% SDS.

Cross-linking of PTA-1 Antigen—Jurkat-PTA-1 cells (5×10^7 cells/treatment) or CHO-PTA-1 cells (1×10^7 cells/treatment) were harvested by centrifugation or with trypsin-versene solution, respectively, washed with culture medium, and then resuspended in 1 ml of medium containing 10 μg of LeoA1 or control mAb for 15 min at room temperature. After washing, the cells were either cross-linked with 10 μg of RAM in 1 ml of medium or incubated in medium alone for 15 min at room temperature. The cells were washed with cold PBS before lysis and processing for SDS-PAGE analysis.

Immunoisolation of Plasma Membrane Fragments—The method described by Harder and Kuhn (62) was used with slight modifications. Briefly, LeoA1 (anti-PTA-1) and OKT3 (anti-CD3) mAbs were coupled to M-450 sheep anti-mouse magnetic beads (Dynal), according to the manufacturer's instructions. Jurkat-PTA-1 cells (3×10^7 cells/treatment) were incubated with either the PTA-1- or CD3-coupled beads for 0, 5, and 10 min at 37 °C and then immediately pelleted at 4 °C. The bead-cell conjugates were washed in H buffer (10 mM Hepes, pH 7.2, 250 mM sucrose, 2 mM $MgCl_2$, 10 mM NaF and 1 mM vanadate supplemented with Complete™ protease inhibitors) and then resuspended in 1 ml of H buffer containing 0.2 mM pervanadate prior to homogenization of the cells on ice with a glass Dounce homogenizer. The homogenates were washed with cold H buffer, and the beads were isolated with a magnet (Dynal), and this was repeated three times. After the final wash, the proteins were eluted from the beads with reducing Laemmli sample buffer, separated by SDS-PAGE, and analyzed by immunoblotting.

Yeast Two-hybrid Assay—All MATCHMAKER yeast two-hybrid vectors and cDNA libraries were purchased from Clontech (Palo Alto, CA), with the exception of the GAL4 DNA binding domain vector, pGBT9LacZ (a gift of Dr. I. Macreadie, Biomolecular Research Institute, Parkville, Australia). pGBT9LacZ contains a Trp-selectable marker and a GAL4-responsive *lacZ* gene (*i.e.* additional to that contained in the yeast chromosome), which allows for highly sensitive detection of interacting proteins by increasing the production of β-galactosidase. The cytoplasmic tail and part of the transmembrane region of PTA-1 (aa 266–336) was amplified by PCR from human PTA-1 cDNA using the forward 5′-gttgtttgaattctcaattacc-3′ and reverse 5′-gcataaagatccctgcaggagtac-3′ oligonucleotide primers and subcloned to pGBT9LacZ using the introduced EcoRI and PstI restriction endonuclease sites (underlined). The PTA-1 S329F mutant was generated by PCR amplification of the PTA-1 cDNA using the above forward primer with a reverse primer 5′-ctgcagttaaactctagtctttggtctgcgaAagaaggttgg-3′ containing the Ser to Phe mutation (mismatched oligonucleotide bases are represented in capital letters), along with an introduced PstI site, and then subcloned to the pGBT9LacZ vector. Similarly, the PTA-1 S329A mutant was constructed using the same forward primer with a reverse primer containing the Ser to Ala mutation, followed by subcloning to pGBT9LacZ (provided by Dr. P. Sherrington, University of Liverpool, UK). The PTA-1 S329D mutant was generated using the QuikChange™ site-directed mutagenesis kit (Stratagene, La Jolla, CA), with the oligonucleotide pairs 5′-gtcaactatccaaccttcGAtcgcagaccaaagac-3′ and 5′-gtctttggtctgcgaTCgaaggttggatagttgac-3′, both containing the Ser to Asp mutation, with pGBT9LacZ-PTA-1 as template. All constructs were validated by automated DNA sequencing using an ABI Prism 377 Automated DNA Sequencer. The MATCHMAKER cDNA expression libraries were cloned into GAL4 activation domain vectors containing a leucine (Leu) selectable marker. They consisted of a human leukemia library produced from unstimulated Jurkat T cell mRNA containing 2×10^6 clones, cloned into the pGAD10 vector; the second was a human brain library encompassing 5×10^6 clones in the pACT2 vector.

Transformation and analysis of *Saccharomyces cerevisiae* HF7c strain was performed according to the manufacturer's recommended protocol (Clontech). Briefly, the yeasts were sequentially transformed with pGBT9LacZ-PTA-1 and the pGAD10-Jurkat or pACT2-brain cDNA libraries using the lithium acetate method and plated onto synthetic medium lacking Leu, Trp, and His but containing 15 mM 3-aminotriazole (Sigma) and a mixture of galactose, glycerol, and ethanol as the carbon source. After 4–5 days at 30 °C, colonies were lifted onto nitrocellulose (MSI, Westbro, MA), incubated facing upward on fresh medium for 24 h, and, following liquid nitrogen treatment, assayed for β-galactosidase activity by incubation with 5-bromo-4-chloro-3-indolyl-β-D-galactopyranoside (X-gal) substrate. pGAD10/pACT2 constructs from His-positive/β-galactosidase-positive colonies were isolated from the yeast and recovered by electroporation into JM109 cells. Following small scale plasmid purifications, the cDNAs of potential interactors were identified by automated DNA sequencing. These constructs were then reintroduced into the yeast and rescreened for their ability to interact with pGBT9LacZ-PTA-1 and were quantified using the liquid β-galactosidase assay. For further two-hybrid analysis, pGBT9LacZ-PTA-1 mutants S329F, S329A, and S329D were screened against the identified pGAD10-4.1G and assayed as above.

λ *Phage cDNA Library Screen*—A Jurkat T cell cDNA library was used, which was constructed in the EcoRI site of the λ phage vector λgt10 (Clontech) and represented 1.1×10^6 independent clones. The phage were plated on *Escherichia coli* Y1090 strain and screened by plaque hybridization. The DNA probe consisted of the 4.1G cDNA insert isolated from the yeast two-hybrid library screen, labeled using a high prime DNA labeling kit (Roche Applied Science). Hybond N membrane (Amersham Biosciences) lifts were performed in duplicate and were composed of denaturation (1.5 M NaCl, 0.5 M NaOH) for 7 min, neutralization (1.5 M NaCl, 0.5 M Tris-HCl, pH 7.5) for 5 min twice, and a 2× SSC rinse followed by UV cross-linking. The membranes were incubated in prehybridization/hybridization solution (50% formamide, 5× SSC, 5× Denhardt's solution, 0.1% SDS, 50 mM $NaPO_4$, pH 6.5, 5 μg of herring sperm DNA) for 2 h at 42 °C prior to overnight hybridization with the ^{32}P-labeled 4.1G probe at 42 °C. The filters were washed twice at room temperature in 2× SSC, 0.1% SDS and then in 0.2× SSC, 1% SDS for 60 min at 55 °C, followed by autoradiography. Positive plaques were isolated from the original plate, and the bacteriophage eluted in PSB (0.1 M NaCl, 10 mM $MgCl_2$, 10 mM Tris-HCl, pH 7.4, 0.05% gelatin) overnight at 4 °C. Secondary and tertiary screens were performed to facilitate the isolation of a single positive clone. The bacteriophage particles were purified from the PSB eluate, and the DNA was isolated according to standard procedures. The cDNA insert was released from the phage vector by EcoRI restriction, subcloned to pBluescript vector (Promega Corp., Madison, WI), followed by automated DNA sequencing.

Northern Blot Analysis—Northern blotting was performed as previously described (54), using total RNA isolated from either resting Jurkat cells or Jurkat cells treated with TPA at 50 ng/ml overnight to induce PTA-1 expression. The DNA probe consisted of the 4.1G cDNA insert isolated from the yeast two-hybrid screen and radiolabeled as described above (see λ phage library screen). Following autoradiography, the filter was reprobed for glyceraldehyde-3-phosphate dehydrogenase as an RNA loading control.

Immunofluorescent Cell Staining and Confocal Microscopy—CHO-PTA-1 cells were grown on glass coverslips overnight and then fixed and permeabilized with cold methanol for 10 min at −20 °C. Dual color immunostaining was performed with LeoA1 mAb and 4.1G-Head and 4.1G-Tail polyclonal antibodies as indicated, followed by detection with a mixture of Alexa 488-conjugated goat anti-mouse and Alexa 594-conjugated goat anti-rabbit immunoglobulins (Molecular Probes, Inc., Eugene, OR). The stained coverslips were mounted onto glass slides with Prolong™ Antifade reagent (Molecular Probes), and the fluorescently labeled cells were visualized on a Zeiss LSM510 confocal microscope.

For the cytochalasin D experiments, CHO-PTA-1 and CHO-DAF cells were used. Cells were grown on glass coverslips and treated with either 2 μM cytochalasin D (Sigma) or carrier alone (Me_2SO) for 60 min at 37 °C, followed by fixation with 4% formaldehyde (w/v) in PBS for 15 min at room temperature and permeabilization with 0.3% Triton X-100 in PBS for 5 min at room temperature. The cells were stained with monoclonal (LeoA1 and VIIIA7) or polyclonal (4.1G-Head) antibodies, followed by Alexa 594-conjugated goat anti-mouse or anti-rabbit immunoglobulins (Molecular Probes), with actin visualized with Alexa 488-conjugated phalloidin (Molecular Probes). The coverslips were mounted as above and examined by epifluorescent microscopy on a Zeiss Axioplan microscope. The merged images were obtained by overlaying the

individual images using Adobe Photoshop™ software.

Construction, Expression, and Purification of GST Fusion Proteins—The GST-PTA-1 construct containing the PTA-1 carboxyl terminus and part of the transmembrane region (aa 266–336) was generated by subcloning the EcoRI restriction fragment from pGBT9LacZ-PTA-1 to pGEX-2T (Amersham Pharmacia Biotech). The GST-PTA-1ΔTRV construct also contains the same region of PTA-1 but lacks the three carboxyl-terminal residues Thr, Arg, and Val (aa 266–333), subcloned to pGEX-4T-3 using EcoRI/NotI restriction sites (provided by Dr. P. Sherrington). The GST-4.1G-Tail (GST-4.1G-CTD) construct containing the 175 carboxyl-terminal residues (aa 830–1005) was prepared from EcoRI restriction of pGAD10–4.1G subcloned to pGEX-2T. The GST-4.1G-Head construct comprising the 115 amino-terminal residues (aa 1–115) was prepared by PCR amplification of pCDNA3–4.1G-myc (provided by Dr. P. Gascard, University of California, Berkeley, CA), using the oligonucleotides 5′-gaagtaggatccgtgtctgaag-3′ and 5′-ggggaattcttatctaagacc-3′, and subcloned to pGEX-2T via the introduced BamHI/EcoRI restriction sites. The GST-RBD construct encodes a GST fusion to the Rap binding domain (provided by Dr. J. Bos, Utrecht University, The Netherlands) and has been previously described (63). All constructs were verified by restriction endonuclease analysis or automated DNA sequencing.

BL21 (DE3) cells (Stratagene) were transformed with the various GST constructs, cultured to an A_{600} of 0.6- 1.0, and recombinant GST fusion protein expression was induced with 0.1 mM isopropyl-1-thio-β-D-galactopyranoside for 4 h. The bacteria were collected by centrifugation, resuspended in ice-cold PBS containing Complete™ protease inhibitors (Roche Applied Science), and then disrupted by sonication on ice for 6 × 10-s pulses. Triton X-100 was added (1% final) and mixed for 30 min at 4 °C, and the soluble and insoluble proteins were separated by centrifugation at 3000 × *g* for 10 min. The recombinant GST proteins were purified from the soluble supernatant by incubation with PBS-washed glutathione-Sepharose 4B beads (Amersham Biosciences) at 4 °C for 2 h. The GST-bead complexes were then washed three times with PBS. For the pull-down experiments, the GST-bead complexes were further washed with lysis buffer prior to incubation with cell lysates. For recombinant GST protein purification, the GST proteins were eluted with five bed volumes of glutathione elution buffer (10 mM reduced glutathione in 50 mM Tris-HCl, pH 8, supplemented with Complete™ protease inhibitors) at 4 °C, and the beads were removed by centrifugation. The eluted proteins were evaluated for purity and integrity by SDS-PAGE and quantified by spectrophotometry.

GST Pull-down Assay—For some experiments, Jurkat cells were biosynthetically labeled with [^{35}S]cysteine/methionine prior to lysis. The cells were pelleted, washed in cysteine/methione-free RPMI (Thermo Trace, Melbourne, Australia), and then starved in the same medium for 30 min at 37 °C. The cells were then resuspended in this medium with the addition of 1 mCi of [^{35}S]cysteine/methionine (PerkinElmer Life Sciences) for 3 h at 37 °C, and TPA (50 ng/ml) stimulation was continued through the labeling as appropriate. After washing with PBS, the cells were lysed for 60 min at 4 °C with Nonidet P-40 lysis buffer (1% Nonidet P-40, 25 mM Tris, pH 7.6, 150 mM NaCl supplemented with Complete™ protease inhibitors).

The protein kinase C (PKC) assay kit (Stratagene) was used to phosphorylate GST-PTA-1, according to the manufacturer's instructions. Briefly, the GST-PTA-1-Sepharose bead complexes were washed in the supplied phosphorylation buffer and then incubated in this buffer containing 1 mM rATP, diolein and phosphatidyl serine phospholipids, and PKC (α, β, and γ isoforms) for 10 min at 30 °C. The protein-bead complexes were washed in radioimmune precipitation assay lysis buffer and then used in the pull-down assay.

Unless indicated otherwise, Jurkat cells were lysed with radioimmune precipitation assay lysis buffer for 60 min at 4 °C. Insoluble material was removed by centrifugation for 10 min at 14,000 × *g* at 4 °C. Lysates were precleared using GST-alone-coupled Sepharose beads for 1–2 h at 4 °C and then pulled down with either GST-, PTA-1-, phosphorylated PTA-1-, or PTA-1ΔTRV-coupled beads as indicated for 1–2 h at 4 °C. The beads were then washed four times in lysis buffer, eluted with reducing Laemmli sample buffer, and resolved by SDS-PAGE. Gels containing radiolabeled samples were fixed, Coomassie-stained, and dried, and the labeled protein bands were visualized by fluorography. Otherwise, gels were transferred to nitrocellulose and subjected to immunoblotting.

Immunoprecipitation—Approximately 1.5 × 10^8 Jurkat-PTA-1 cells were treated with TPA (50 ng/ml) for 2 h at 37 °C and then treated with 2 mM cytochalasin D for 60 min at 37 °C. The cells were pelleted and washed with PBS prior to digitonin (Sigma) lysis (1% digitonin, 20 mM Hepes, pH 7.5, 150 mM NaCl, with Complete™ protease inhibitors) for 60 min at 4 °C before clarification by centrifugation 14,000 × *g*. To reduce nonspecific binding during immunoprecipitation, the lysate was precleared with the capture reagents alone. Antigens were then immunoprecipitated with the specific mAbs (LeoA1; 2D3, a control antibody that binds to CD47 on the surface of Jurkat cells) indirectly bound by rabbit anti-mouse immunoglobulins (DAKO) directly coupled to CnBr-activated Sepharose 4B beads (Amersham Biosciences). Immunocomplexes were then washed four times with the digitonin lysis buffer and then eluted by boiling with reducing Laemmli sample buffer. Samples were resolved by 7.5% SDS-PAGE, transferred to nitrocellulose, and then analyzed by immunoblotting.

Surface Plasmon Resonance—The BIACore experiments were performed essentially as described previously (64). In brief, purified GST and GST-4.1G-Head or Tail (CTD) protein (50 mg/ml) were immobilized onto CM5 sensor chips (BIACore™) by the amine coupling method, according to the manufacturer's instructions. The immobilization yielded 3000 (GST) and 6300 (GST-4.1G-Head, similarly for GST-4.1G-Tail) resonance units of binding. Purified GST-PTA-1, GST-4.1G-Tail, and GST-alone proteins (all at 50 μg/ml) were passed over the sensor chips. The very weak binding of GST was subtracted from the GST-PTA-1 and GST-4.1G-Tail binding to yield the resultant sensorgram.

RESULTS

PTA1 Is Recruited into Membrane Rafts and Associates with Rap1 and the Cytoskeleton upon Cross-linking—A physical and functional association between PTA-1 and LFA-1 integrin suggested that PTA-1 may be implicated in the adhesive processes that occur during T cell activation. Many of the molecules that engage in the T cell signaling cascade are found to localize in or be recruited to lipid rafts during the activation process (8). To examine whether PTA-1 might be contained within rafts, we used the biochemical approach of isolating the cold Triton X-100-insoluble material known as GEMs or detergent-insoluble glycolipid structures that may represent raft material (Fig. 1*A*). Resting T lymphocytes and Jurkat T cells express very little PTA-1 protein (54); therefore, to facilitate protein detection, we utilized Jurkat cells stably transfected with PTA-1 for these assays. However, similar results were obtained with non-transfected Jurkat cells that had been prestimulated for 30 h with TPA to induce PTA-1 protein expression and then rested overnight before restimulation (data not shown; see below). In these assays, a proportion of PTA-1 from resting cells was found to localize to the GEM fraction (*G* in Fig. 1*A*), indicating raft-resident status; however, cross-linking of the PTA-1 antigen with anti-PTA-1 mAb followed by rabbit anti-mouse antibody (PTA-1 + RAM) (Fig. 1*A*) or stimulation of the cells with TPA (Fig. 1*B*) induced an increased proportion of the PTA-1 to locate to the GEM fraction. The endoplasmic reticulum-resident protein, calnexin, was used as a control in these experiments and was found predominantly in the soluble fraction (*S*) as expected; its distribution was not altered by cell stimulation (Fig. 1*B*). In these experiments, it was also found that cross-linking of PTA-1 resulted in an accumulation of this antigen in the washed cytoskeletal pellet that had precipitated through the sucrose gradient (*I*; Fig. 1*A*).

Upon cross-linking or cell stimulation with TPA or anti-CD3, PTA-1 becomes phosphorylated on a serine residue and associates with LFA-1 (58, 59). Subsequent LFA-1 engagement and cross-linking results in the tyrosine phosphorylation of PTA-1 and its association with Lyn PTK (59). These data implicate PTA-1 in both the regulation of LFA-1 function and further downstream signaling. Recent work has strongly implicated Rap1 in the regulation of LFA-1 function (22), and in the transfected Jurkat cells, we found Rap1 to be a resident of GEMs (Fig. 1*B*); therefore, we considered whether PTA-1 might associate with Rap1. The use of GST-PTA-1 in pull-down experiments did not reveal any direct association (data not shown); therefore, we employed the method developed by Harder and Kuhn (62) to analyze plasma membrane subfragments for associated signaling molecules. Magnetic beads were

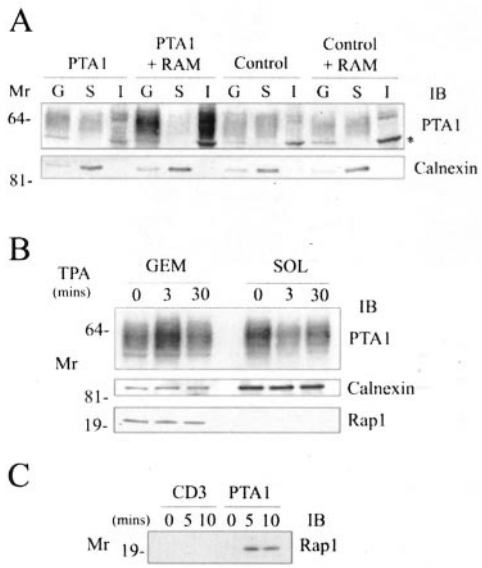

FIG. 1. **Cross-linking of PTA-1 results in recruitment to GEMs and an association with the cytoskeleton and with Rap1-containing plasma membrane fragments.** *A*, Jurkat cells stably transfected with PTA-1 were treated with mAb (anti-PTA-1 or control) alone or by further cross-linking with rabbit anti-mouse antibodies (anti-PTA-1 + RAM; control + RAM) for 15 min before lysis in cold Triton X-100 and centrifugation through a sucrose gradient. Immunoblotting (*IB*) for PTA-1 was performed on equal protein loadings of the visible GEM band (*G*) and the soluble material (*S*) containing the bulk of the protein, together with an equivalent proportion of the washed insoluble cytoskeletal pellet (*I*). Note that the soluble fraction contains over 90% of the total protein content; therefore, because of equal protein loading, PTA-1 contained in this fraction is greatly diluted and yields a low signal. Note also that PTA-1 is represented by the diffuse band at around 64 kDa; the tight band *below* (*) is a nonspecific band that was sometimes observed in immunoblots for PTA-1. As a control, identical samples were immunoblotted for the endoplasmic reticulum protein calnexin. *B*, PTA-1-transfected Jurkat cells were stimulated with TPA as indicated, and cell lysates were separated on sucrose gradients as in *A*. The GEM fractions and protein equivalents of the soluble fractions were immunoblotted for PTA-1, calnexin, and Rap1. *C*, immunoblotting for Rap1 shows association with the plasma membrane fragments immunoisolated with anti-PTA-1-coated magnetic beads but not with anti-CD3-coated beads after 5 and 10 min of cross-linking at 37 °C.

coated with the anti-PTA-1 mAb, LeoA1, or, as a control, with anti-CD3. These were mixed with PTA-1-transfected Jurkat cells and warmed at 37 °C for 5 or 10 min before homogenization of the cells and immunoisolation of the bound membrane fragments. Analyzed by immunoblotting, the CD3 fragments co-purified with several signaling molecules after 5 and 10 min of cell stimulation (62) (data not shown) but not with Rap1 (Fig. 1*C*). In contrast, stimulation and immunoprecipitation with the anti-PTA-1 (LeoA1)-coated beads revealed that Rap1 co-associates with PTA-1 in membrane fragments isolated from the transfected Jurkat cells after PTA-1 cross-linking (Fig. 1*C*). This result places Rap1 in the vicinity of PTA-1 and LFA-1 at the plasma membrane of these cells; other signaling molecules associated with the complex will be reported elsewhere.

The Cytoplasmic Domain of PTA-1 Binds the Carboxyl-terminal Domain (CTD) of Protein 4.1G—Yeast two-hybrid analysis was then used to identify PTA-1 binding partners that might contribute to complex formation. The entire cytoplasmic region and part of the transmembrane domain of PTA-1 in the bait vector (Fig. 2*A*) was used to screen a Jurkat T cell cDNA library. The entire library of 2×10^6 independent clones was screened, and three positive clones were isolated. All three clones were confirmed as true binding partners when tested against a range of controls. The three clones were sequenced and shown to contain the same sequence identified as identical to the CTD of protein 4.1G (Fig. 2*B*), a ubiquitous member of the protein 4.1 family (65). The relative strength of binding between PTA-1 and the CTD of 4.1G was measured in a liquid β-galactosidase assay, and the well characterized CD4-Lck interaction was measured as a comparative control; CD4-Lck interaction produced 2.9 β-galactosidase units, and the PTA-1–4.1G produced 91.4 units, indicating strong binding in the yeast two-hybrid assay. To further validate this result and to identify additional binding partners, we used the same region of PTA-1 to screen a second cDNA library. A human brain library was selected, because PTA-1 is also expressed in certain brain tissues,[2] and 11 positive clones were isolated from screening 5×10^6 clones. Validation tests confirmed only one of these clones to be a true positive, and this was found to encode exactly the same protein as those isolated from the Jurkat library. Isolation of this same clone validates the interaction between PTA-1 and the CTD of 4.1G in this assay, since the same protein was obtained from four separate clones and two different libraries.

Parra *et al.* (65) record that protein 4.1G is generally expressed in a wide range of tissues but is relatively less abundant than 4.1R in hematopoietic tissues and only weakly expressed in peripheral leukocytes; therefore, we examined the expression of 4.1G mRNA in Jurkat cells by Northern blot analysis. Fig. 2*C* shows that 4.1G mRNA in these cells appears as three major transcripts, at approximately 4.1, 4.6, and 7.3 kb. This is very similar to the pattern reported for human brain but quite different from that obtained in seven other human tissues where a single prominent transcript at around 5 kb was obtained (65). The multiple brain transcripts were attributed to alternative splicing and/or differential use of polyadenylation sites (65), and in support of alternative splicing in Jurkat cells we isolated a cDNA from this cell line that showed apparent differential exon usage from the published sequence of 4.1G assembled from various EST clones (65) (GenBank™ accession number AY512660). Since the expression of PTA-1 in Jurkat cells is induced by TPA at the transcriptional level (65), we also examined the influence of TPA on the isoforms of 4.1G expressed in these cells. Fig. 2*C* illustrates that this treatment resulted in the down-regulation of the larger transcripts, leaving only the 4.1-kb transcript.

In order to examine 4.1 protein expression, rabbit antibodies ("tail" antibodies) were raised and affinity-purified against the CTD of 4.1G in the form of a GST fusion protein and used for Western blot analyses. These analyses confirmed the presence of 4.1G protein in the Jurkat cells and also in the CHO cells used for some immunofluorescent staining experiments (Fig. 2*D*). The major products identified from the Jurkat cells were at around 170 kDa, and a lesser band was seen at around 111 kDa. The largest band approximates in size to the major product identified from transfected COS cells by Parra *et al.* (65) and is larger than the size of ~113 kDa predicted from the cDNA. These different products possibly could exhibit some post-translational processing, and a smaller band at ~110 kDa was also illustrated by Parra *et al.* (65) in their transfected COS cell analysis. Fig. 2*D* from the Jurkat cell lysate also reveals the presence of a series of polypeptides ranging from 30 to 173 kDa; whether these represent alternatively spliced products or proteolytic products is not known, but this pattern was highly reproducible in numerous experiments. Similar results were obtained with CHO cell lysates analyzed in the same way (Fig. 2*D*), although some of the bands differed in M_r from those of the Jurkat cells. This wide range in polypeptide size was not entirely unexpected, since 4.1 proteins are reported to display

[2] G. F. Burns, unpublished data.

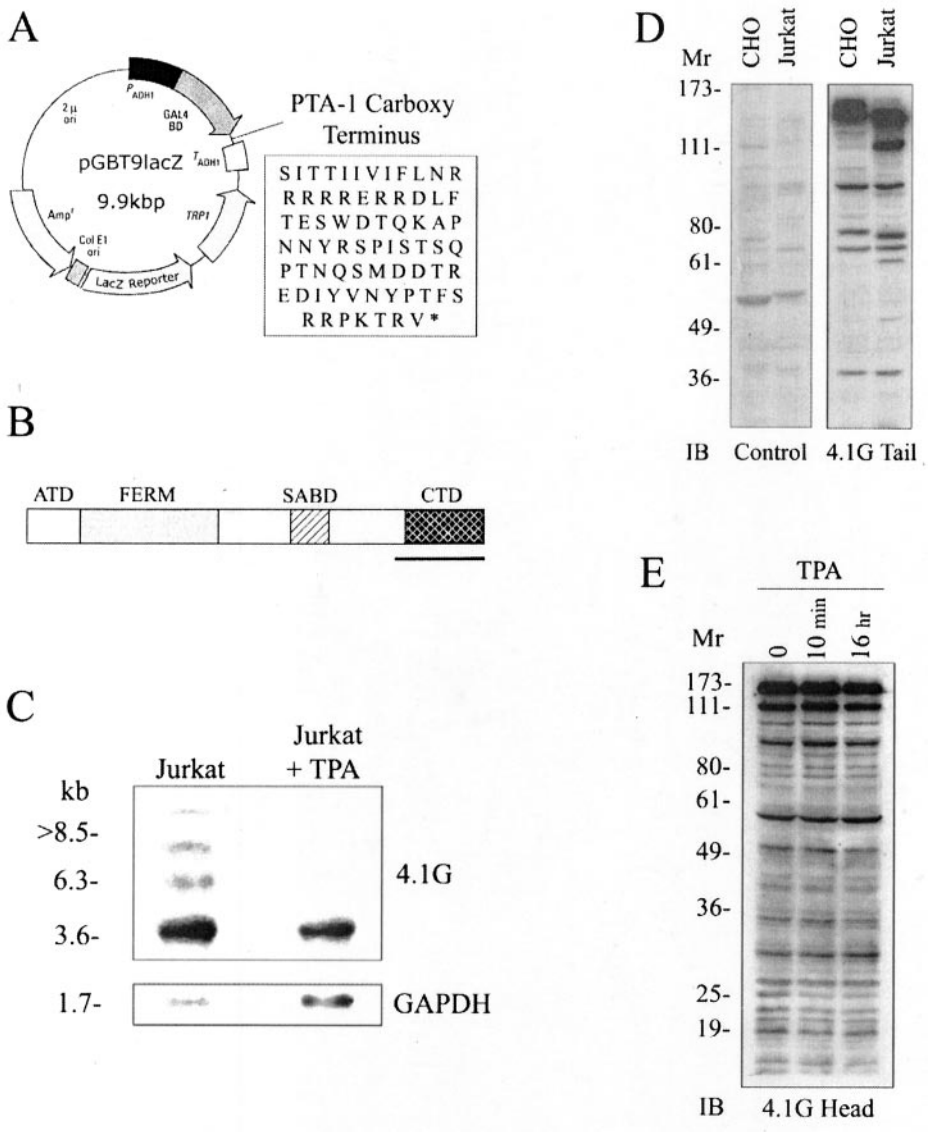

FIG. 2. **The cytoplasmic domain of PTA-1 interacts with the carboxyl-terminal domain of 4.1G that is expressed in Jurkat T cells.** *A*, depiction of the amino acid sequence of PTA-1 incorporated into the pGBT9LacZ Y2H bait vector. *B*, schematic of 4.1G showing the major functional domains. *SABD*, spectrin actin-binding domain. The position of the 4.1G cDNA clones isolated in the two-hybrid assays against PTA-1 are *underlined*. *C*, Northern blot for 4.1G in resting Jurkat cells and Jurkat cells stimulated with TPA overnight. The filters were stripped and reprobed for glyceraldehyde-3-phosphate dehydrogenase (*GAPDH*). *D*, immunoblot (*IB*) of CHO and Jurkat cell lysates with preimmune rabbit serum (control) or with affinity-purified rabbit antibodies raised against the CTD of 4.1G (4.1G-Tail). *E*, immunoblot of Jurkat cell lysates with affinity-purified antibodies raised against the ATD of 4.1G (4.1G-Head). Cells were untreated (*0*) or stimulated with TPA for 10 min or 16 h before analysis.

extensive diversity in molecular weight, with one Western blot study revealing 4.1 immunoreactive proteins ranging in size from 30 to 210 kDa (66). Nevertheless, because the CTD of 4.1G bound by PTA-1 in the yeast two-hybrid system that was also used for immunization shares some 60% identity with the same region of 4.1R, it was important to establish that each of the immunoreactive bands represented 4.1G and not cross-reactive 4.1R or another 4.1 family member. To accomplish this, rabbit antibodies were raised and affinity-purified against a GST fusion protein incorporating only the first 115 aa residues that are unique to 4.1G ("head" antibody). Used directly for Western blotting of Jurkat (Fig. 2*E*) or CHO (data not shown) cell lysates or in reciprocal immunoprecipitation and blotting experiments, both the "head" and the "tail" antibodies yielded similar results, thereby validating the status of the multiple 4.1G polypeptides (Fig. 2, compare *D* and *E*); however, in immunofluorescent experiments with CHO cells, the "tail" but not the "head" antibodies did exhibit intranuclear staining, indicating some 4.1R immunoreactivity (data not shown). In the blotting experiments with both "head" (Fig. 2*E*) and "tail" (data not shown) antibodies, it was found that stimulation of the Jurkat cells with TPA did not alter the profile of putative isoforms obtained (Fig. 2*E*).

We then utilized these antibodies to seek to identify a physical *in vivo* association between PTA-1 and 4.1G. CHO cells stably transfected with PTA-1 were used in these experiments, and good co-localization was seen at the plasma membrane between PTA-1 and 4.1G detected with either "head" or "tail" antibodies (Fig. 3*A*). Protein 4.1 contains a spectrin/actin-binding domain and might be expected to associate with actin, particularly at the submembranous skeleton at the plasma membrane. To visualize this, permeabilized transfected CHO cells were incubated with Alexa 488-phalloidin to illuminate F actin and also stained for 4.1G (Fig. 3*B*). Some degree of co-localization was obtained, but this was much more evident after the actin cables were disrupted by treatment with cytochalasin D causing the fibers to collapse into a pronounced lumpy appearance. After such treatment, 4.1G staining was found to be coincident with the areas of condensed actin (Fig. 3*B*). Co-staining of cells for DAF (CD55) did not reveal coincidence of staining with phalloidin before or after cytochalasin treatment, whereas staining for PTA-1 showed close coincidence of staining with phalloidin after treatment (Fig. 3*B*).

It was noted above that upon antibody-mediated cross-linking of PTA-1 on Jurkat cells, a proportion of the PTA-1 was found to precipitate with the cytoskeleton (see Fig. 1*A*). Therefore, we questioned whether this might also occur in the transfected CHO cells and, if so, whether this distribution of 4.1G

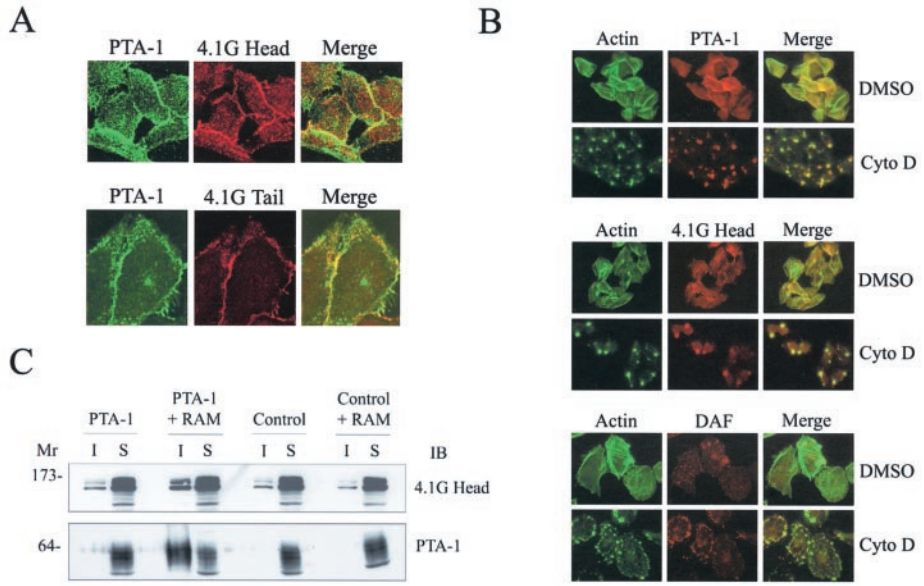

FIG. 3. **Association between PTA-1 and 4.1G in PTA-1-transfected CHO cells.** *A*, confocal analysis was performed on the PTA-1-transfected CHO cells labeled by indirect immunofluorescence for PTA-1 with the mouse mAb LeoA1 (*green*) and either the 4.1G-Head or 4.1G-Tail affinity-purified rabbit antibodies (*red*). *B*, immunofluorescent images obtained from the PTA-1-transfected CHO cells, co-stained for actin with phalloidin (*green*) together with PTA-1 (mAb LeoA1) and 4.1G (rabbit Head antibody) or co-stained for DAF (mAb VIIIA7) before or after treatment of the cells with 2 μM cytochalasin D for 60 min at 37 °C prior to fixation. *DMSO*, Me_2SO. *C*, CHO transfectants were cross-linked with the indicated antibodies as described in the legend to Fig. 1*A*. Following centrifugation of the post nuclear supernatants at 14,000 $\times$ *g* for 15 min, immunoblot (*IB*) analyses were then performed on the insoluble pellet (*I*) and soluble fraction (*S*).

was also influenced by such cross-linking. PTA-1-transfected CHO cells were treated with anti-PTA-1 mAb (or control) and then cross-linked with RAM before lysis and centrifugation of the postnuclear supernatant to isolate the cytoskeletal pellet. Immunoblotting for PTA-1 showed that after specific cross-linking a large proportion of the PTA-1 antigen now pelleted with the cytoskeleton, indicating a tight association (Fig. 3*C*). Reblotting the same samples for 4.1G revealed that a proportion of this protein pelleted with the cytoskeleton in the resting CHO cells; however, this proportion was increased following cross-linking of PTA-1 (Fig. 3*C*). These results show that cross-linking of PTA-1 on the cell surface can influence the distribution of 4.1G, further substantiating an association between the molecules.

The Carboxyl-terminal Peptide of PTA-1 Binds the MAGUK, Human Discs Large—As we documented in the Introduction, members of the protein 4.1 family are found to associate with MAGUKs, which play an important role in assembling signal transduction complexes at the interface of the membrane cytoskeleton (67). MAGUKs contain one or more PDZ domains that engage in protein-protein interactions, including binding to the carboxyl-terminal peptides of some transmembrane proteins. The carboxyl terminus of PTA-1 terminates in the sequence Lys-Thr-Arg-Val (KTRV), a recognized PDZ-binding motif; therefore, we determined whether this region of PTA-1 engaged in protein binding. For this, we prepared GST fusion proteins encoding the entire cytoplasmic tail of PTA-1 or the PTA-1 tail lacking the three terminal residues, TRV (PTA-1ΔTRV). These were used in pull-down experiments with lysates of resting or TPA-stimulated Jurkat cells that had been prelabeled with [^{35}S]Cys/Met. The fluorographs obtained revealed several polypeptides that bound to GST-PTA-1 but not to GST alone (Fig. 4*A*), indicating specific binding. Comparison of the specific bands precipitated by PTA-1 *versus* PTA-1ΔTRV identified several differences, including one polypeptide at around 21 kDa that, intriguingly, was more prominent in the PTA-1ΔTRV precipitate (Fig. 4*A*). The identity of this band is not known, but this result indicates that the carboxyl-terminal peptides can influence PTA-1-protein binding, possibly either by direct binding to a PDZ-containing protein that blocks binding to another site or by virtue of a particular conformation. Two bands in particular were prominent in the PTA-1 pull-downs that were negligible or absent in the pull-downs with PTA-1ΔTRV; notably, these bands were also more prominent from lysates of Jurkat cells that had been stimulated with TPA-1 (Fig. 4*A*).

Either of these two bands might represent binding to a PDZ-containing protein, and we focused on the band at around 110 kDa (Fig. 4*A*, *arrow*) because this approximates the migration of hDlg in SDS-PAGE, and hDlg has been shown to associate with protein 4.1R in epithelial cells (52). Further pull-down experiments were therefore carried out with the PTA-1 and PTA-1ΔTRV proteins and tested by immunoblotting for hDlg; in addition, since PKC-mediated phosphorylation of PTA-1 has been implicated in its function (68), we also tested binding to the GST-PTA-1 protein that had been subjected to PKC-mediated phosphorylation *in vitro* (+*PKC*). The results obtained are shown in Fig. 4*B*, where it is apparent that GST-PTA-1 can bind to hDlg. Binding is modestly increased after phosphorylation of the GST-PTA-1 by PKC, but removal of the terminal TRV peptide residues from PTA-1 almost abolishes binding of hDlg, with the small residual binding perhaps being attributable to a ternary complex (Fig. 4*B*). To confirm that PTA-1 associates with hDlg *in vivo*, we carried out co-precipitation analyses from TPA-stimulated Jurkat PTA cells analyzed by Western blotting and established that precipitation of PTA-1 co-precipitates hDlg; however, the co-association signal was very faint (data not shown), possibly because the associated molecules were being lost by prior precipitation with the cytoskeleton. In support of this, when co-immunoprecipitations were carried out after pretreatment of the cells with cytochalasin D to disrupt the actin cytoskeleton, clear co-association was obtained (Fig. 4*C*).

Next we examined whether hDlg was localized in the GEM fraction representing membrane rafts and whether its distribution in the transfected Jurkat cells was altered following TPA treatment or cross-linking of PTA-1 (Fig. 5). PTA-1-transfected Jurkat cells were left untreated or stimulated with TPA for 3 or 30 min before cell lysis and centrifugation through sucrose gradients to isolate the GEM fraction. The isolated GEM fractions were run in SDS-PAGE together with equal protein loading from the soluble fractions (Fig. 5*A*) and then immunoblotted for hDlg and also 4.1G (head), PTA-1, and, as a control, calnexin. The results (Fig. 5*B*) indicated that hDlg is a resident of rafts; the proportion of the protein found in the GEM fraction did not increase upon treatment of the cells with TPA but actually appeared to decrease without material becoming apparent in the soluble fraction, probably indicating

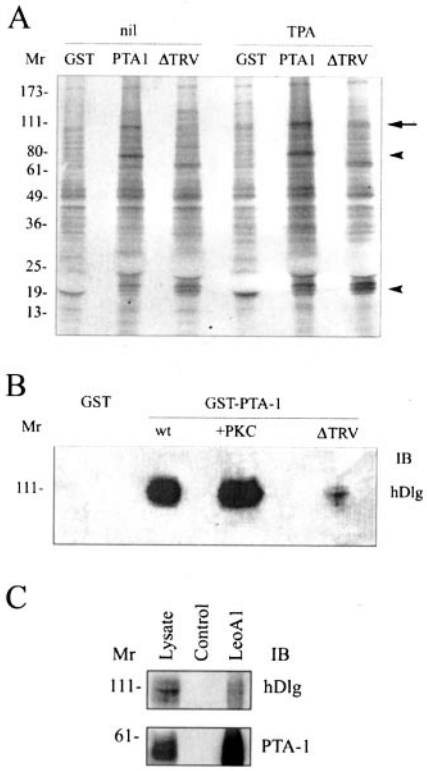

FIG. 4. **PTA-1 associates with hDlg.** *A*, fluorograph of ^{35}S-labeled proteins precipitated with GST alone, GST-PTA-1 fusion protein, or GST-PTA-1 fusion protein lacking the three carboxyl-terminal amino acid residues (ΔTRV). For the pull-down assay, Nonidet P-40 lysates were prepared from Jurkat cells biosynthetically labeled with [^{35}S]cysteine/methionine, either from resting cells or after overnight treatment with TPA. The *arrow* and *arrowheads* indicate three protein species of interest. *B*, Jurkat cells were treated with TPA for 2 h before lysis with radioimmune precipitation assay. Cell lysates were used in pull-down assays against either GST, GST-PTA-1, GST-PTA-1 *in vitro* phosphorylated with PKC, or GST-PTA-1ΔTRV, and samples were analyzed for hDlg association by immunoblotting (*IB*). *C*, hDlg co-immunoprecipitated with PTA-1. Jurkat-PTA-1 permanent transfectants were stimulated with TPA for 2 h and treated with cytochalasin D, and the soluble digitonin lysate was incubated with anti-PTA-1 mAb (LeoA1) or control mAb and RAM-Sepharose beads. Immunoprecipitated proteins were immunoblotted for PTA-1 and hDlg. The lysate sample represents 1% of the total lysate.

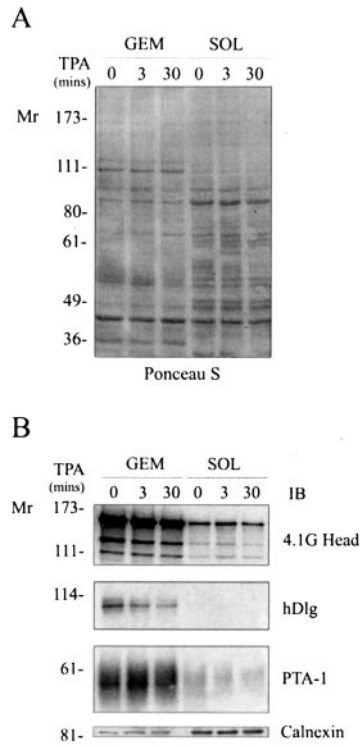

FIG. 5. **Localization of PTA-1, 4.1G, and hDlg in the GEM fraction.** Jurkat-PTA-1 transfected cells were treated with TPA for the indicated times and subjected to cold Triton X-100 lysis, and the GEM fraction was separated by centrifugation through a sucrose gradient. Equivalent total protein from each of the GEM and soluble (*SOL*) fractions were run on SDS-PAGE and transferred to nitrocellulose. *A*, Ponceau S staining of the membrane illustrating equal protein loading. *B*, the membrane illustrated in *A* was subjected to immunoblotting (*IB*) analysis for 4.1G-Head, PTA-1, and hDlg. These three proteins were seen to be enriched in the GEM fraction, whereas a control blot for calnexin showed enrichment in the soluble fraction.

loss of hDlg to the pelleted cytoskeleton. In these assays, both 4.1G and PTA-1 were identified predominantly in the GEM fractions, whereas calnexin located to the soluble fractions (Fig. 5*B*). Experiments using PTA-1 cross-linking in which the cytoskeletal pellet also was analyzed showed that hDlg was prominent in this fraction as well as the GEM fraction, although the relative distribution of hDlg was not altered by cross-linking (data not shown).

The PDZ-binding Peptide at the Carboxyl Terminus of PTA-1 Influences Binding to Multiple Isoforms of 4.1G—As we noted above, the cytoplasmic tail of PTA-1 can be phosphorylated by PKC after treatment of Jurkat cells or platelets with TPA. The residue that is phosphorylated in this way was identified by Shibuya *et al.* (59) as serine 329 toward the carboxyl terminus of PTA-1, within the last 8 residues (FS^{329}RRPKTRV) and adjacent to the putative PDZ-binding peptide identified by us. Shibuya *et al.* (59) mutated this serine residue to phenylalanine (Ser → Phe) and recorded that this mutation abrogated PTA-1 phosphorylation in response to TPA treatment of transfected murine thymoma cells and also that these cells were no longer able to mediate PTA-1-mediated cell adhesion; the authors concluded from these data that phosphorylation of Ser^{329} plays a critical role in PTA-1-mediated adhesion and signaling. We therefore tested whether Ser^{329} might be implicated in PTA-1 binding to 4.1G. Table I shows a representative yeast two-hybrid binding analysis of the interaction between the CTD of protein 4.1G, the cytoplasmic region of PTA-1, and mutations of PTA-1 in which Ser^{329} was mutated to either phenylalanine (Ser → Phe) or alanine (Ser → Ala). As shown in Table I, measured in β-galactosidase units, it is apparent that substitution of the serine at 329 with phenylalanine reduced the strength of binding in this assay but still permitted strong binding to occur. Substitution of this serine residue with alanine did not significantly reduce the PTA-1–4.1G interaction. From these analyses, we conclude that whereas Ser^{329} within PTA-1 may be implicated in binding to the CTD of protein 4.1G, such involvement is more likely to result from the conformation of PTA-1 in this region rather than an involvement of serine phosphorylation, since the bulky phenylalanine residue caused more disruption than alanine as a substitute. In support of this interpretation, we found that substitution of Ser^{329} with aspartate (Ser → Asp) to mimic phosphoserine did not alter the strength of PTA-1–4.1G interaction in the β-galactosidase assay (data not shown). It is interesting to note that the Ser → Phe substitution that still binds to CTD of 4.1G in the context of the PTA-1 cytoplasmic tail now has the sequence FFRR, similar to the FFKR sequence within the α subunit of LFA-1 that is central to the regulation of integrin adhesive function (69, 70); should this region be directly implicated in the PTA-1–4.1G binding interaction, then it is possible that LFA-1 also could bind to the CTD of 4.1G.

Intermolecular binding by members of the ternary complex

TABLE I
Quantitative yeast two-hybrid analysis of the interaction between mutations of PTA-1 and the CTD of 4.1G

S. cerevisiae HF7c cells were co-transformed as described under "Experimental Procedures." Protein interactions were tested by growth in selective liquid SD medium lacking Trp for the single transformants, Leu and Trp (−LT) for the double transformants, or Leu, Trp, and His with the inclusion of 3-aminotriazole (−LTH) for higher stringency and then quantified using a liquid β-galactosidase assay. The strong interaction between the cytoplasmic tail of PTA-1 and the 4.1G CTD under both selective conditions was decreased with Ser → Phe mutation and to a lesser degree in the Ser → Ala mutation, but binding to the 4.1CTD was still significant and well above levels of activation using the control activation domain pTD1 plasmid. The β-galactosidase assay was performed in triplicate with the values presented as the mean ± S.E.

Sample	β-Galactosidase units
PTA1 alone	0.99 ± 0.22
Ser → Phe alone	0.62 ± 0.40
Ser → Ala alone	0.29 ± 0.07
PTA1 + 4.1G −LT	85.41 ± 13.33
Ser → Phe + 4.1G −LT	23.72 ± 3.30
Ser → Ala + 4.1G −LT	70.95 ± 3.81
PTA1 + 4.1G −LTH	216.56 ± 76.49
Ser → Phe + 4.1G −LTH	97.16 ± 12.97
Ser → Ala + 4.1G −LTH	168.01 ± 26.44
PTA1 + pTD1	3.34 ± 1.72
Ser → Phe + pTD1	10.18 ± 6.03
Ser → Ala + pTD1	1.24 ± 0.51

of erythrocytes, between 4.1R, the MAGUK, p55, and the transmembrane protein, glycoprotein C, is interdependent and dynamic; for example, the affinity of binding between glycophorin C and p55 is increased by an order of magnitude by 4.1R in *in vitro* binding assays (43). Therefore, we utilized the GST fusion proteins PTA-1 and PTA-1ΔTRV and also *in vitro* phosphorylated GST-PTA-1 in pull-down assays immunoblotted for 4.1G to determine whether the putative PTA-1-hDlg-4.1G complex might be similarly interdependent (Fig. 6).

For these experiments, we used lysates from Jurkat cells that had been left untreated or stimulated for 3 min, 10 min, 2 h, or overnight with TPA. Initially, we concentrated on examining immunoblots of the higher molecular weight material, around the major 4.1G 170-kDa isoform identified in whole cell lysates. An example of these blots is shown in Fig. 6*A*, and similar results were obtained by immunoblotting with the "tail" antibody from lysates from both unstimulated and TPA-stimulated Jurkat cells (data not shown). It is apparent that whereas there is a degree of specific pull-down by the PTA-1 fusion proteins compared with GST alone, there are no differences between PTA-1 and PTA-1ΔTRV; nor is there any relative enrichment of this 4.1G isoform in the pull-downs compared with the total lysate.

A totally different profile was obtained when we examined the pull-downs of lower molecular weight isoforms of 4.1G (Fig. 6*B*). Several bands were prominent in the PTA-1 fusion protein pull-downs that were absent in the GST-alone track, and some were apparently greatly enriched compared with the whole lysate blot. The *arrowheads* in Fig. 6*B* point to bands that were consistently seen to be enriched in the PTA-1 fusion protein pull-downs; these bands were identified with both the "tail" antibody (Fig. 6*B*) and the "head" antibody (data not shown), indicating that they represent 4.1G isoforms and not proteolytic breakdown products, and each of the identified isoforms appeared to be equally represented in lysates from unstimulated or TPA-stimulated Jurkat cells (Fig. 6*B*, *a* and *b*). Of particular interest were the bands identified at around 55 and 35 kDa (*asterisk on arrowhead* in Fig. 6*B*). The isoform at ~55 kDa was poorly represented in the total cell lysates and strongly precipitated by each of the PTA-1-GST fusion proteins, but the pull-down with PTA-1ΔTRV yielded more of this product than native or phosphorylated PTA-1 (Fig. 6*B*). This result perhaps indicates that interaction between PTA-1 and a PDZ-containing protein reduces the association between PTA-1 and the 55-kDa isoform of 4.1G. The opposite was the case with the 35-kDa isoform pulled down by native and phosphorylated PTA-1 but not by PTA-1ΔTRV. In this instance, the binding of

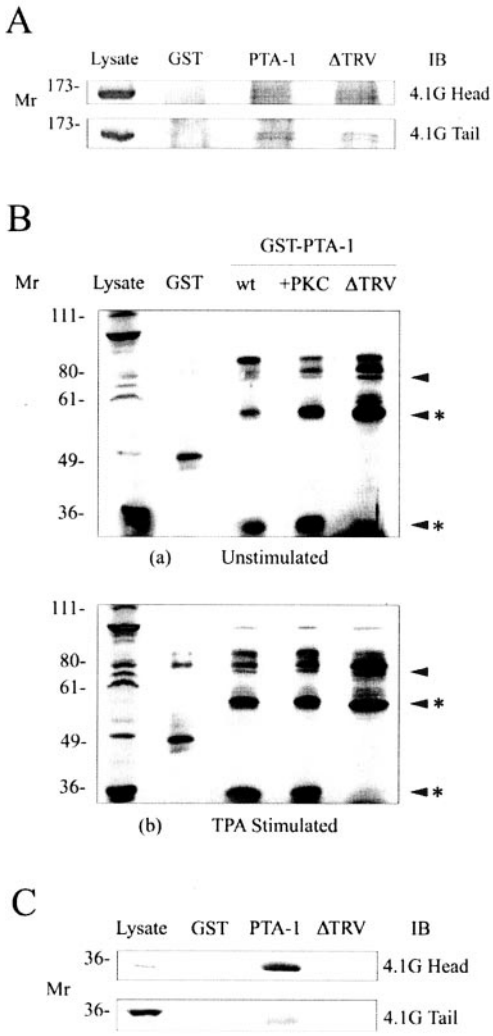

FIG. 6. **Binding of PTA-1 to various isoforms of 4.1G is influenced by the three carboxyl-terminal amino acid residues of PTA-1.** *A*, binding of PTA-1 to the 170-kDa isoform of 4.1G is not influenced by the terminal TRV peptide. Resting Jurkat cell lysates were incubated with either GST alone, GST-PTA-1, or GST-PTA-1ΔTRV, and precipitated proteins were separated by SDS-PAGE and immunoblotted (*IB*) with the 4.1G-Head or -Tail rabbit antibodies. The control lysate sample represents 0.5% of the total lysate. *B*, the terminal TRV peptide of PTA-1 influences the association with small 4.1G isoforms. Resting Jurkat cells (*a*) or Jurkat cells stimulated with TPA for 2 h (*b*) were subjected to cold radioimmune precipitation assay lysis and then incubated with either GST, GST-PTA-1 (*wt*), GST-PTA-1 phosphorylated with PKC *in vitro* (*+PKC*), or GST-PTA-1 lacking the three terminal amino acids (Δ*TRV*). Resultant proteins precipitated were run on SDS-PAGE and immunoblotted with the 4.1G-Tail rabbit antibody. The lysate sample constitutes ~1% of the total. The *arrowheads* indicate the 4.1G isoforms that the PTA-1 fusion proteins consistently precipitate. The *bands* further highlighted with *asterisks* indicate the influence of the terminal TRV peptide of PTA-1 in the association with 4.1G isoforms. Note that in *a* and *b* in the Δ*TRV lane*, there is the false appearance of a band at ~35 kDa, caused by the label bound by the GST protein used in the pull-down diffusing into this region. *C*, GST pull-down experiment, as described in *A*, illustrating the lower 4.1G isoform pulled down by the GST-PTA-1 fusion protein. Note that the 4.1G-Head antibody recognizes the lower 4.1G isoform at 35 kDa, which the GST-PTA-1 precipitates, whereas the 4.1G-Tail antibody illuminates this band plus a stronger larger band above.

a PDZ-containing protein may be required for binding to this small isoform of protein 4.1G. Note that in Fig. 6*B*, the immunoblot of the whole lysate appears to identify a prominent band in the same position as the 35-kDa isoform pulled down by PTA-1. However, this band, which actually migrates slightly slower than the PTA-1-associated band, is not the same polypeptide, since this band is not illuminated with the "head" antibody, whereas the associated band is identified by both the "head" and "tail" antibodies (Fig. 6*C*). Therefore, this isoform too represents a minor 4.1G product that is greatly enriched by binding to PTA-1 in pull-down experiments.

The Amino-terminal Region of 4.1G Binds to PTA-1 from Activated Cell Lysates—Despite the association between PTA-1 and 4.1G documented in numerous assays above, in repeated attempts we were unable to demonstrate an association between PTA-1 from cell lysates and the 4.1G CTD used as a GST fusion protein. The reasons for this are not clear, but it was not readily attributable to interference by another binding protein, since we obtained no detectable direct binding between GST-PTA-1 and GST-4.1G.CTD in surface plasmon resonance experiments (data not shown). In further pull-down experiments with GST fusion proteins, we also sought to identify an association between PTA-1 and activated Rap1 by pull-down with the Rap binding protein (20), followed by immunoblotting for PTA-1. These also gave a negative result, but for these experiments we had used the GST-4.1G-Head protein as an additional control and obtained the unexpected result that this unique domain of 4.1G was able to pull down PTA-1 from lysates of activated but not resting Jurkat cells (Fig. 7). The example shown in Fig. 7*A* shows the pull-down of PTA-1 obtained from Jurkat cells that had been either pretreated with TPA for 30 h to induce PTA-1 protein expression and then rested overnight (*Nil*) before treatment with the anti-PTA-1 mAb (LeoA1) alone, with anti-PTA-1 cross-linked with RAM antibody, or with TPA to induce activation. Western blotting for PTA-1 shows that this protein was precipitated by the GST-4.1G "head" protein after the Jurkat cells had been stimulated by antibody-mediated cross-linking (Fig. 7*A*, *track 10*) or by treatment with TPA (Fig. 7*A*, *track 14*). These results indicate that upon activation of the Jurkat cells, PTA-1 undergoes some change enabling it to bind the amino-terminal region of 4.1G; this change could be in consequence of a direct conformational change in PTA-1, perhaps mediated by phosphorylation or lipid association, or by an association between PTA-1 and another molecule such as hDlg. Alternatively, activation of the Jurkat cells could cause a conformational change to a PTA-1-binding protein such that it is no longer able to bind, thus freeing PTA-1 to bind to the head region of 4.1G. To begin to discriminate between these different possibilities, we carried out direct binding experiments between GST-PTA-1 and GST-4.1G "head" proteins by surface plasmon resonance. The results obtained from these BIAcore experiments (Fig. 7*B*) show that these two GST-fusion proteins can interact directly. From this, we can conclude that the cytoplasmic tail of PTA-1 can bind to the "head" region of 4.1G without the requirement for amino acid modification or binding to an intermediary protein.

Taken together, we believe that the simplest interpretation of the different 4.1 binding data obtained in this report is that in the resting cell, PTA-1 constitutively associates with the CTD of 4.1G. Because of the relative excess of 4.1G protein over PTA-1 in these cells (witnessed in immunofluorescent staining and immunoprecipitation experiments (data not shown)), PTA-1 in the cell lysate is unable to bind exogenously presented 4.1G.CTD in the form of a GST fusion protein. There are likely also to be conformational constraints, since GST-PTA-1 and GST-4.1G.CTD did not bind directly in surface plasmon resonance experiments (data not shown); but direct binding was indicated within the context of yeast cells, and GST-PTA-1 was able to precipitate multiple isoforms of 4.1G from lysates of resting Jurkat cells (Fig. 6). Upon cell activation, we propose, there is induced a conformational change in 4.1G, perhaps analogous to that which occurs in ERM proteins (38), that alters the conformation of the CTD of 4.1G and exposes a PTA-1 binding region in the head domain. These dynamic associations, together with an association with hDlg, provide a structural basis for a regulated protein complex at the T cell surface with links to the cytoskeleton.

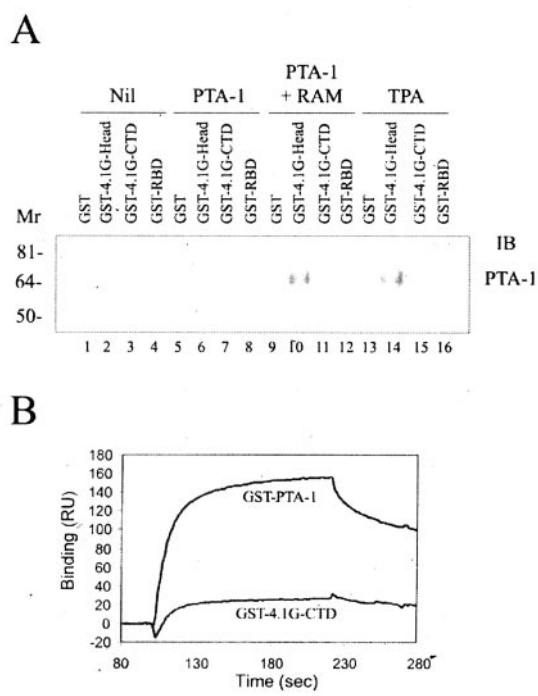

FIG. 7. **PTA-1 associates with the amino-terminal domain (Head) of 4.1G.** *A*, Jurkat cells were treated with TPA for 30 h to induce PTA-1 protein and then rested overnight (*Nil*), treated with the anti-PTA-1 mAb LeoA1 alone (*PTA-1*), treated with LeoA1 cross-linked with rabbit anti-mouse antibody (*PTA-1 + RAM*), or treated with TPA for 40 min at room temperature (*TPA*) to induce activation. Cell lysates were then incubated with GST alone, GST-4.1G-Head (amino-terminal domain), GST-4.1G-CTD (carboxyl-terminal domain), or GST-RBD (Rap1 binding domain) and then precipitated with glutathione-Sepharose beads. The protein eluates were separated by SDS-PAGE, transferred to nitrocellulose, and immunoblotted (*IB*) for PTA-1. Upon activation either by cross-linking (PTA-1 + RAM) or by TPA stimulation, PTA-1 associated with the amino-terminal domain of 4.1G (*lanes 10* and *14*, respectively). *B*, surface plasmon resonance sensorgram showing the binding between PTA-1 and the 4.1G-Head domain. Purified GST alone, GST-PTA-1, and GST-4.1G-CTD were passed over GST-4.1G-Head- or GST-coupled sensor chips. After subtraction of the weak binding of the GST fusion proteins to the GST-coupled chip, significant binding of GST-PTA-1 to the GST-4.1G-Head coupled chip was observed, in comparison with the weak binding of GST-4.1G-CTD. No binding was observed for GST (data not shown).

DISCUSSION

Here we present evidence for a direct physical association between a T cell activation antigen, PTA-1, a protein 4.1 family member, 4.1G, and a MAGUK, human discs large. Since the related protein 4.1R also binds hDlg (71), it is possible that PTA-1 forms a ternary complex with 4.1G and hDlg, redolent of other 4.1-transmembrane protein-MAGUK ternary complexes that form important functional units serving as a clustering apparatus at sites of cell-cell communication (41). The reported physical and functional association between PTA-1 and LFA-1 (59), together with its involvement in the development of cytotoxic T cells from their precursors (55), suggests that such a

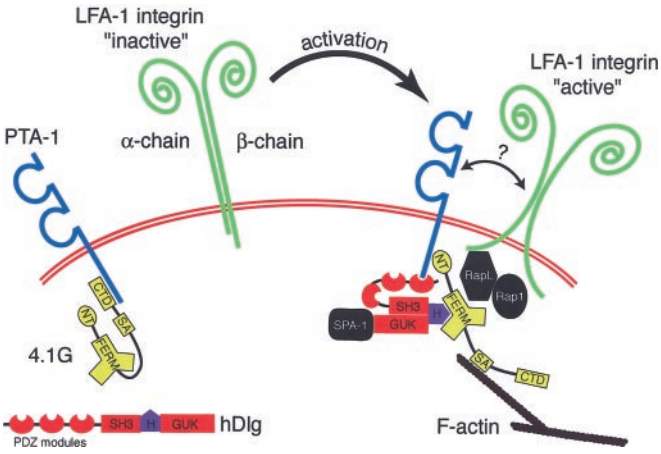

FIG. 8. **Model of the dynamic assembly of the LFA-1-PTA-1 complex.** In the resting state, PTA-1 forms an association with the CTD of the FERM superfamily protein 4.1G. 4.1G consists of a unique amino-terminal extension (*NT*), the three-lobed FERM domain, a spectrin-actin (*SA*) binding domain, and a CTD. As shown, 4.1G is possibly present in a closed conformation, resulting from an intramolecular interaction between its amino and carboxyl termini which is characteristic of the FERM superfamily proteins. The LFA-1 integrin is present in an inactive form and not associated with PTA-1. Upon activation, a ternary complex between PTA-1, hDlg, and 4.1G is formed where the cytoplasmic tail of PTA-1 now associates with the amino-terminal extension domain of 4.1G, and its carboxyl-terminal PDZ-binding peptide binds to one of the PDZ modules in the MAGUK protein, hDlg. The HOOK (*H*) domain of hDlg in turn associates with the FERM domain of 4.1G. In this model, the CTD and SA binding domain of 4.1G are now exposed and may facilitate further molecular interactions, such as the association with F-actin. Activated LFA-1 may also physically associate with the PTA-1 complex via an interaction between their respective extracellular domains. Intracellularly, this complex may be regulated by interaction with the Rap1-GTPase and its related signaling components. The integrin α-chain cytoplasmic domain possesses a consensus motif that may support binding of the Rap1 effector molecule RapL. Additionally, the guanylate kinase (*GUK*) domain of hDlg is known to bind the Rap1-activating protein, SPA-1. These interactions are suggested to play a regulatory role in the assembly of the LFA-1-PTA-1 complex (diagram adapted from Ref. 52). The NH_2-terminal domain of hDlg is not shown for simplicity. See "Discussion" for further details.

complex may play an important functional role at the immunological synapse. A model incorporating this putative complex is given in Fig. 8.

There are, however, substantial differences between the molecular interactions described for the other known ternary complexes involving a transmembrane protein in association with 4.1 proteins and that described here for PTA-1. Thus, in the best characterized example, involving the transmembrane protein glycophorin C, the MAGUK, p55, and protein 4.1R, both the cytoplasmic domain of glycoprotein C and the HOOK domain of p55 bind to the FERM domain of 4.1R at adjacent sites (72). By contrast, the cytoplasmic domain of PTA-1 binds to the CTD of protein 4.1G, as determined in yeast two-hybrid assays, and to the amino-terminal domain (ATD) of 4.1G, at least in activated cells, as shown in GST fusion protein pull-down assays and by surface plasmon resonance. Note that the ATD used in these assays incorporated only the first 115 residues of 4.1G, a region that is unique to this protein 4.1 family member and does not incorporate any of the downstream FERM domain (see Fig. 2*B*). The function of these domains of 4.1 family members is unknown. The CTD of protein 4.1G has been shown to bind to the immunophilin-binding protein, FKBP13, that may function as a molecular chaperone to catalyze the folding and/or assembly of proteins in the endoplasmic reticulum (73), and to an intracellular loop of the A1 adenosine receptor (74). In addition, the CTD of nuclear forms of the paralogues 4.1N and 4.1R have been demonstrated to bind to and to be implicated in the functioning of a nuclear GTPase that regulates phosphatidylinositol 3-kinase kinase activity and the nuclear mitotic apparatus protein, respectively (75, 76). The ATD of 4.1R contains a high affinity calcium-dependent calmodulin binding domain (77); however, this region of 4.1G shares only 23% identity over the 17 residues involved (73); therefore, it is unclear whether such a functional domain is present in 4.1G. To our knowledge, PTA-1 is the first protein identified as binding the unique head region of 4.1G.

We show that PTA-1 also binds the MAGUK, hDlg, probably through binding to a PDZ domain. This finding potentially places PTA-1 as a membrane anchor for a large multimeric complex incorporating a diversity of functional entities, each with the capacity to modify the immunological response. hDlg comprises a series of modules that bind to a bewildering number of proteins. The protein additionally undergoes multimerization that could contribute to clustering (67). The proline-rich amino-terminal domain of hDlg interacts with Lck protein tyrosine kinase. This is followed by three PDZ domains known to bind the potassium ion channel, Kv1.3, and the tumor suppressor PTEN among others (47, 78); a Src homology 3 domain; and then a HOOK domain able to bind the FERM domain of 4.1R. Whether this interaction also occurs between hDlg and 4.1G has not been established, but this is likely to be the case, since the FERM domains of these paralogues are highly homologous, and, at least in epithelial cells, this interaction plays a critical role in recruiting hDlg to the lateral membrane (52). At the carboxyl terminus of hDlg is a guanylate kinase-like domain, the hallmark of MAGUK family members. This domain is enzymically inactive and seems to have evolved as a specialized protein recognition module. The guanylate kinase domain of hDlg has been shown to bind to the Rap1 GTPase-activating protein known as SPA-1, SPAL, or SPAR that plays a role in regulating cell adhesion (44, 45, 79). This domain also binds to the kinesin-like motor protein known as GAKIN, and in T lymphocytes (Jurkat T cells) the hDlg-GAKIN complex moves from the cytoplasm to the lymphocyte cap, presumably along microtubules, upon stimulation by antibody-mediated cross-linking to induce cell activation (46). GAKIN-mediated transport of hDlg is dependent upon its molecular motor domain, and Asaba *et al.* (51) have proposed that hDlg is a cargo molecule of GAKIN that is directed to specialized sites of cell-cell contact by the microtubule plus end-directed motor protein. Adding to the potential size of the complex is the range of partners known to associate with protein 4.1 family members by binding to the FERM domain; these include Ca^{2+}-calmodulin, phosphatidylinositol 4-phosphate, and phosphatidyl 4,5-biphosphate and transmembrane proteins such as CD44 (41), and it has been suggested that this domain is likely also to bind several GTPase protein regulators (41, 80).

The FERM domains of 4.1G and 4.1R share 76% identity (65); therefore, it is likely that 4.1G also has several binding partners in this region. Whether any of these 4.1/hDlg binding molecules also co-associate with a PTA-1 complex is not known, but since several can be located to rafts at the immunological synapse, it seems possible that such multimeric complexes will be formed. This possibility raises the interesting questions of where the complex(es) are formed and how the existence of such a PTA-1-associated complex might influence LFA-1 binding and signaling.

We favor the hypothesis that the 4.1G-associated complexes are formed at recycling rafts found in the Golgi region (81). Parra *et al.* (65) demonstrated that 4.1G is concentrated in the perinuclear region in transfected COS cells, and we show here that 4.1G, hDlg, and PTA-1 are concentrated in the GEM fraction that represents raft material. The composition of the

raft material would promote clustering and protein-protein associations, and, in association with growing microtubules, the complex could be delivered to specific areas at the leading edge (82), perhaps driven by GAKIN. Alonso and Millán (83) have recently provided a detailed consideration of the role of rafts in the assembly and trafficking of signaling complexes in T cells; they note that in these cells, the uropod is rich in rafts that might provide a reservoir for subsequent delivery of raft proteins and lipids to the immunological synapse. Notably, TCR engagement drives the transport of gangliosides and Lck (which is known to associate with hDlg) (47) from an intracellular store to the plasma membrane and the translocation of Lck-associated PKCθ to rafts at the immunological synapse. Of interest, ICAM-3 that accumulated in the uropod of polarized T cells after delivery by binding to the FERM domain of moesin (34) is subsequently targeted to sites of immune cell-cell contact by an unknown mechanism (10). The similarities between the FERM domains among 4.1 superfamily members might allow ICAM-3 at the uropod to interact with 4.1G for transport back to the leading edge. Similarly, the FERM domain of 4.1G potentially could interact with the β subunit of LFA-1 (29), thereby providing a mechanism for the documented association with PTA-1 (59). However, Shibuya *et al.* (59) noted that PTA-1 associated specifically with LFA-1 after T cell activation rather than with all β_2 integrins as would be the case if β_2 interacted with the 4.1G FERM domain. In this regard, the recent work of Katagiri *et al.* (84) may be instructive. These authors identified a Rap1 effector termed RAPL that binds to Rap1 and also to LFA-1 dependent upon two charged residues just downstream of the FFKR motif in the integrin α subunit. Importantly, they showed that in T cells RAPL was localized to a perinuclear region in the cytoplasm near the microtubule organizing center. LFA-1 also was found localized at this site, and upon T cell stimulation both RAPL and LFA-1 migrated together to the immunological synapse at the leading edge. Mutation of the two charged residues in LFA-1 that interact with RAPL inhibited the redistribution of LFA-1 alone. Katagiri *et al.* (84) also note that Rap1 activation begins in the perinuclear region and suggest that Rap1 and RAPL may be involved in the loading and direction of cargo molecules, including LFA-1, from the perinuclear region to the immunological synapse at the leading edge following T cell activation.

How this redistribution of the complex is achieved is not known, but we suggest that the PTA-1–4.1G-hDlg complex may be implicated. In addition to the activation-induced association between PTA-1 and LFA-1 (59), we show here that T-cell activation also induces an association between PTA-1 and Rap1 in membrane fragments and that both are contained within rafts (Fig. 1). Of interest, deletion of the first 100 residues of RAPL resulted in a protein (RAPΔN) that failed to bind Rap1-GTP yet acted as a dominant-negative inhibitor of Rap1 activation-induced adhesion and also inhibited the redistribution of LFA-1 (84). We note that contained within this region of RAPL is the sequence REKNCLGMKLSED that approximates to a consensus 4.1 binding sequence RXKX_{0-4}GXYX_3E (where X represents any amino acid) identified by Hoover and Bryant (41). Whether these proteins can associate awaits further study, but the existence of such a complex together with hDlg and GAKIN would provide a satisfactory explanation for several aspects of LFA-1 trafficking and regulation.

Acknowledgments—We thank Sonja Stojko, Ke Chen, and Maja Hadzic for excellent technical assistance and Maxine Zerafa for administrative assistance in the preparation of the manuscript and figures. We also thank Drs. Mohini Lutchman and Athar Chishti for providing the anti-hDlg mAb, Drs. Philippe Gascard and John Conboy for the pCDNA3–4.1G-myc construct, and Dr. Johannes Bos for supplying the GST-RBD protein.

REFERENCES

1. Boussiotis, V. A., Freeman, G. J., Berezovskaya, A., Barber, D. L., and Nadler, L. M. (1997) *Science* **278,** 124–128
2. Grakoui, A., Bromley, S. K., Sumen, C., Davis, M. M., Shaw, A. S., Allen, P. M., and Dustin, M. L. (1999) *Science* **285,** 221–227
3. Delon, J., and Germain, R. N. (2000) *Curr. Biol.* **10,** 923–933
4. Khan, A. A., Bose, C., Yam, L. S., Soloski, M. J., and Rupp, F. (2001) *Science* **292,** 1681–1686
5. Tordjman, R., Lepelletier, Y., Lemarchandel, V., Cambot, M., Gaulard, P., Hermine, O., and Romeo, P. H. (2002) *Nat. Immunol.* **3,** 477–482
6. Simons, K., and Toomre, D. (2000) *Nat. Rev.* **1,** 31–39
7. Miceli, M. C., Moran, M., Chung, C. D., Patel, V. P., Low, T., and Zinnanti, W. (2001) *Semin. Immunol.* **13,** 115–128
8. Baldari, C. T., Telford, J. L., and Acuto, O. (2000) *EMBO J.* **19,** 4857–4865
9. Dustin, M. L., and Cooper, J. A. (2000) *Nature* **1,** 23–29
10. Montoya, M. C., Sancho, D., Bonello, G., Collette, Y., Langlet, C., He, H. T., Aparicio, P., Alcover, A., Olive, D., and Sanchez-Madrid, F. (2002) *Nat. Immunol.* **3,** 159–168
11. Juan, M., Vinas, O., Pino-Otin, M. R., Places, L., Martinez-Caceres, E., Barcelo, J. J., Miralles, A., Vilella, R., de la Fuente, M. A., Vives, J., Yagüe, J., and Gayà, A. (1994) *J. Exp. Med.* **179,** 1747–1756
12. Dustin, M. L., and Springer, T. A. (1989) *Nature* **341,** 619–624
13. Hogg, N., Henderson, R, Leitinger, B., McDowall, A., Porter, J., and Stanley, P. (2002) *Immunol. Rev.* **186,** 164–171
14. Krauss, K., and Altevogt, P. (1999) *J. Biol. Chem.* **274,** 36921–36927
15. Leitinger, B., and Hogg, N. (2002) *J. Cell Sci.* **115,** 963–972
16. Marwali, M. R., Rey-Ladino, J., Dreolini, L., Shaw, D., and Takei, F. (2003) *Blood* **102,** 215–222
17. Porter, J. C., Bracke, M., Smith, A., Davies, D., and Hogg, N. (2002) *J. Immunol.* **168,** 6330–6335
18. Waterman-Storer, C. M., Worthylake, R. A., Liu, B. P., Burridge, K., and Salmon, E. D. (1999) *Nat. Cell Biol.* **1,** 45–50
19. Zhou, X., Li, J., and Kucik, D. F. (2001) *J. Biol. Chem.* **276,** 44762–44769
20. Reedquist, K. A., Ross, E., Koop, E. A., Wolthuis, R. M., Zwartkruis, F. J., van Kooyk, Y., Salmon, M., Buckley, C. D., and Bos, J. L. (2000) *J. Cell Biol.* **148,** 1151–1158
21. De Bruyn, K. M., Rangarajan, S., Reedquist, K. A., Figdor, C. G., and Bos, J. L. (2002) *J. Biol. Chem.* **277,** 29468–29476
22. Katagiri, K., Hattori, M., Minato, N., and Kinashi, T. (2002) *Mol. Cell. Biol.* **22,** 1001–1015
23. Tohyama, Y., Katagiri, K., Pardi, R., Lu, C., Springer, T.A., and Kinashi, T. (2003) *Mol. Biol. Cell.* **14,** 2570–2582
24. Stewart, M. P., McDowall, A., and Hogg, N. (1998) *J. Cell Biol.*, **140,** 699–707
25. Sampath, R., Gallagher, P. J., and Pavalko, F. M. (1998) *J. Biol. Chem.*, **273,** 33588–33594
26. Yan, B., Calderwood, D. A., Yaspan, B., and Ginsberg, M. H. (2001) *J. Biol. Chem.* **276,** 28164–28170
27. Calderwood, D. A., and Ginsberg, M. H. (2003) *Nat. Cell Biol.* **8,** 694–697
28. Chishti, A. H., Kim, A. C., Marfatia, S. M., Lutchman, M., Hanspal, M., Jindal, H., Liu, S. C., Low, P. S., Rouleau, G. A., Mohandas, N., Chasis, J. A., Conboy, J. G., Gascard, P., Takakuwa, Y., Huang, S. C., Benz, E. J. Jr., Bretscher, A., Fehon, R. G., Gusella, J. F., Ramesh, V., Solomon, F., Marchesi, V. T., Tsukita, S., Tsukita, S., and Hoover, K. B. (1998) *Trends Biochem. Sci.* **23,** 281–282
29. Calderwood, D. A., Yan, B., de Pereda, J. M., Alvarez, B. G., Fujioka, Y., Liddington, R. C., and Ginsberg, M. H. (2002) *J. Biol. Chem.* **277,** 21749–21758
30. Krummel, M. F., and Davis, M. M. (2002) *Curr. Opin. Immunol.* **14,** 66–74
31. Shaw, A. S. (2001) *Immunity* **15,** 683–686
32. Roumier, A., Olivo-Marin, J. C., Arpin, M., Michel, F., Martin, M., Mangeat, P., Acuto, O., Dautry-Varsat, A., and Alcover, A. (2001) *Immunity* **15,** 715–728
33. Takahashi, K., Sasaki, T., Mammoto, A., Takaishi, K., Kameyama, T., Tsukita, S., and Takai, Y. (1997) *J. Biol. Chem.* **272,** 23371–23375
34. Serrador, J. M., Alonso-Lebrero, J. L., del Pozo, M. A., Furthmayr, H., Schwartz-Albiez, R., Calvo, J., Lozano, F., and Sanchez-Madrid, F. (1997) *J. Cell Biol.* **138,** 1409–1423
35. Ng, T., Parsons, M., Hughes, W. E., Monypenny, J., Zicha, D., Gautreau, A., Arpin, M., Gschmeissner, S., Verveer, P. J., Bastiaens, P. I., and Parker, P. J. (2001) *EMBO J.* **20,** 2723–2741
36. Pearson, M. A., Reczek, D., Bretscher, A., and Karplus, P. A. (2000) *Cell* **101,** 259–270
37. Hamada, K., Shimizu, T., Matsui, T., Tsukita, S., and Hakoshima, T. (2000) *EMBO J.* **19,** 4449–4462
38. Liddington, R. C., and Bankston, L. A. (2000) *Exp. Cell Res.* **261,** 37–43
39. Hamada, K., Shimizu, T., Yonemura, S., Tsukita, S., Tsukita, S., and Hakoshima, T. (2003) *EMBO J.* **22,** 502–514
40. Nunomura, W., Takakuwa, Y., and Higashi, T. (1997) *J. Biol. Chem.* **272,** 30322–30328
41. Hoover, K. B., and Bryant, P. J. (2000) *Curr. Opin. Cell Biol.* **12,** 229–234
42. Fanning, A. S., and Anderson, J. M. (1999) *Curr. Opin. Cell Biol.* **11,** 432–439
43. Nunomura, W., Takakuwa, Y., Parra, M., Conboy, J., and Mohandas, N. (2000) *J. Biol. Chem.* **275,** 24540–24546
44. Pak, D. T. S., Yang, S., Rudolph-Correia, S., Kim, E., and Sheng, M. (2001) *Neuron* **31,** 289–303
45. Roy, B. C., Kohu, K., Matsuura, K., Yani, H., and Akiyama, T. (2002) *Genes Cells*, **7,** 607–617
46. Hanada, T., Lin, L., Tibaldi, E. V., Reinherz, E. L., and Chishti, A. H. (2000) *J. Biol. Chem.* **275,** 28774–28784
47. Hanada, T., Lin, L., Chandy, K. G., Oh, S. S., and Chishti, A. H. (1997) *J. Biol. Chem.* **272,** 26899–26904
48. Carey, K. D., Dillon, T. J., Schmitt, J. M., Baird, A. M., Holdorf, A. D., Straus, D. B., Shaw, A. S., and Stork, P. J. (2000) *Mol. Cell. Biol.* **20,** 8409–8419
49. Levite, M., Cahalon, L., Peretz, A., Hershkoviz, R., Sobko, A., Ariel, A., Desai,

R., Attali, B., and Lider, O. (2000) *J. Exp. Med.* **191,** 1167–1176
50. Panyi, G., Bagdany, M., Bodnar, A., Vamosi, G., Szentesi, G., Jenei, A., Matyus, L., Varga, S., Waldmann, T. A., Gaspar, R., and Damjanovich, S. (2003) *Proc. Natl. Acad. Sci. U. S. A.* **100,** 2592–2597
51. Asaba, N., Hanada, T., Takeuchi, A., and Chishti, A. H. (2003) *J. Biol. Chem.* **278,** 8395–8400
52. Hanada, T., Takeuchi, A., Sondarva, G., and Chishti, A. H. (2003) *J. Biol. Chem.* **278,** 34445–34450
53. Shibuya, A., Campbell, D., Hannum, C., Yssel, H., Franz-Bacon, K., McClanahan, T., Kitamura, T., Nicholl, J., Sutherland, G. R., Lanier, L. L., and Phillips, J. H. (1996) *Immunity* **4,** 573–581
54. Sherrington, P. D., Scott, J. L., Jin, B., Simmons, D., Dorahy, D. J., Lloyd, J., Brien, J. H., Aebersold, R. H., Adamson, J., Zuzel, M., and Burns, G. F. (1997) *J. Biol. Chem.* **272,** 21735–21744
55. Burns, G. F., Triglia, T., Werkmeister, J. A., Begley, C. G., and Boyd, A. W. (1985) *J. Exp. Med.* **161,** 1063–1078
56. Chen, L. K., Tourvieille, B., Burns, G. F., Bach, F. H., Mathieu-Mahul, D., Sasportes, M., and Bensussan, A. (1986) *Eur. J. Immunol.* **16,** 767–770
57. Jin, B., Scott, J. L., Vadas, M. A., and Burns, G. F. (1989) *Immunology* **66,** 570–576
58. Scott, J. L., Dunn, S. M., Jin, B., Hillam, A. J., Walton, S., Berndt, M. C., Murray, A. W., Krissansen, G. W., and Burns, G. F. (1989) *J. Biol. Chem.* **264,** 13475–13482
59. Shibuya, K., Lanier, L. L., Phillips, J. H., Ochs, H. D., Shimizu, K., Nakayama, E., Nakauchi, H., and Shibuya, A. (1999) *Immunity* **11,** 615–623
60. Jia, W., Liu, X. S., Zhu, Y., Li, Q., Han, W. N., Zhang, Y., Zhang, J. S., Yang, K., Zhang, X. H., and Jin, B. Q. (2000) *Hybridoma* **19,** 489–494
61. Thorne, R. F., Marshall, J. F., Shafren, D. R., Gibson, P. G., Hart, I. R., and Burns, G. F. (2000) *J. Biol. Chem.* **275,** 35264–35275
62. Harder, T., and Kuhn, M. (2000) *J. Cell Biol.* **151,** 199–207
63. Herrmann, C., Horn, G., Spaargaren, M., and Wittinghofer, A. (1996) *J. Biol. Chem.* **271,** 6794–6800
64. Lackmann, M., Bucci, T., Mann, R. J., Kravets, L. A., Viney, E., Smith, F., Moritz, R. L., Carter, W., Simpson, R. J., Nicola, N. A., Mackwell, K., Nice, E. C., Wilks, A. F., and Boyd, A. W. (1996) *Proc. Natl. Acad. Sci. U. S. A.* **93,** 2523–2527
65. Parra, M., Gascard, P., Walensky, L. D., Snyder, S. H., Mohandas, N., and Conboy, J. G. (1998) *Genomics* **49,** 298–306
66. Anderson, R. A., Correas, I., Mazzucco, C., Castle, J. D., and Marchesi, V. T. (1988) *J. Cell. Biochem.* **37,** 269–284
67. Marfatia, S. M., Byron, O., Campbell, G., Liu, S-C., and Chishti, A. H. (2000) *J. Biol. Chem.* **275,** 13759–13770
68. Shibuya, A., Lanier, L. L., and Phillips, J. H. (1998) *J. Immunol.* **161,** 1671–1676
69. Hughes, P. E., Diaz-Gonzalez, F., Leong, L., Wu, C., McDonald, J. A., Shattil, S. J., and Ginsberg, M. H. (1996) *J. Biol. Chem.* **271,** 6571–6574
70. Lu, C. F., and Springer, T. A. (1997) *J. Immunol.* **159,** 268–278
71. Lue, R. A., Marfatia, S. M., Branton, D., and Chishti, A. H. (1994) *Proc. Natl. Acad. Sci. U. S. A.* **91,** 9818–9822
72. Marfatia, S. M., Leu, R. A., Branton, D., and Chishti, A. H., (1995) *J. Biol. Chem.* **270,** 715–719
73. Walensky, L. D., Gascard, P., Fields, M. E., Blackshaw, S., Conboy, J. G., Mohandas, N., and Snyder, S. H. (1998) *J. Cell Biol.* **141,** 143–153
74. Lu, D., Yan, H., Othman, T., Turner, C. P., Woolf, T., and Rivkees, S. A. (2004) *Biochem. J.* **377,** 51–59
75. Mattagajasingh, S. N., Huang, S. C., Hartenstein, J. S., Snyder, M., Marchesi, V. T., and Benz, E. J. (1999) *J. Cell Biol.* **145,** 29–43
76. Ye, K., Hurt, K. J., Wu, F. Y., Fang, M., Luo, H. R., Hong, J. J., Blackshaw, S., Ferris, C. D., and Snyder, S. H. (2000) *Cell* **103,** 919–930
77. Leclerc, E., and Vetter, S. (1998) *Eur. J. Biochem.* **258,** 567–571
78. Adey, N. B., Huang, L., Ormonde, P. A., Baumgard, M. L., Pero, R., Byreddy, D. V., Tavtigian, S. V., and Bartel, P. L. (2000) *Cancer Res.* **60,** 35–37
79. Tsukamoto, N., Hattori, M., Yang, H., Bos, J. L., and Minato, N. (1999) *J. Biol. Chem.* **274,** 18463–18469
80. Wojcik, J., Girault, J-A., Labesse, G., Chomilier, J., Mornon, J-P., and Callebaut, I. (1999) *Biochem. Biophys. Res. Commun.* **259,** 113–120
81. Nichols, B. J., Kenworthy, A. K., Polishchuk, R. S., Lodge, R., Roberts, T. H., Hirschberg, K., Phair, R. D., and Lippincott-Schwartz, J. (2001) *J. Cell Biol.* **153,** 529–541
82. Galjart, N., and Perez, F. (2003) *Curr. Opin. Cell Biol.* **15,** 48–53
83. Alonso, M. A., and Millán, J. (2001) *J. Cell Sci.* **114,** 3957–3965
84. Katagiri, K., Maeda, A., Shimonaka, M., and Kinashi, T. (2003) *Nat. Immunol.* **4,** 741–748

The LFA-1-associated Molecule PTA-1 (CD226) on T Cells Forms a Dynamic Molecular Complex with Protein 4.1G and Human Discs Large

Kylie J. Ralston, Samantha L. Hird, Xinhai Zhang, Judith L. Scott, Boquan Jin, Rick F. Thorne, Michael C. Berndt, Andrew W. Boyd and Gordon F. Burns

J. Biol. Chem. 2004, 279:33816-33828.
doi: 10.1074/jbc.M401040200 originally published online May 11, 2004
